Fast Operator Splitting Methods for Nonlinear PDEs

Zhuolin Qu

Advisor: Prof. Alexander Kurganov

Mathematics Department
Tulane University,New Orleans, LA 70118

April 1, 2016

Outlines

Outlines

The Main Research Question

- To develop highly accurate and efficient methods for nonlinear PDEs that arise in various physical phenomena.

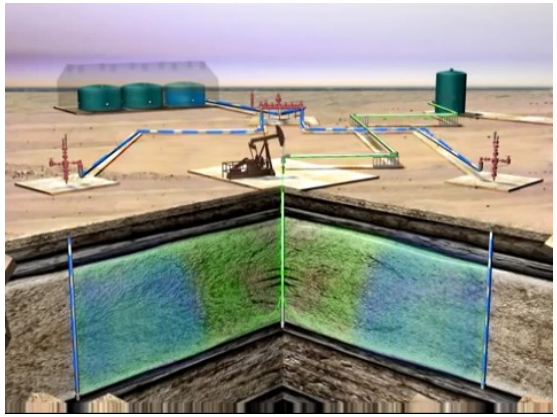

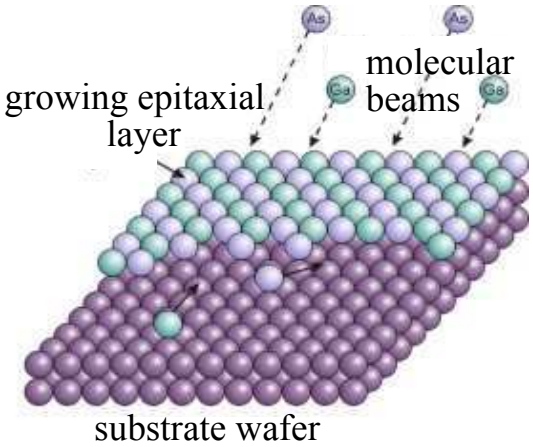

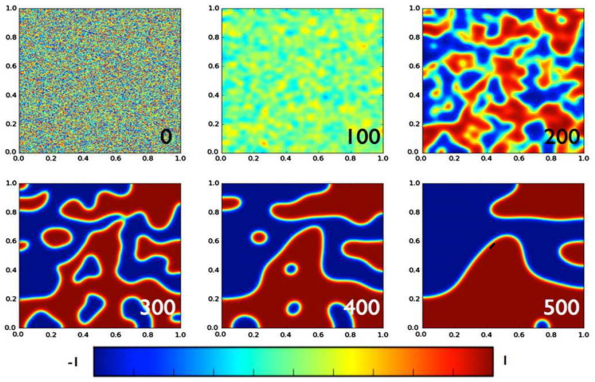

1. Two-phase fluid flow in porous media: $u_t + F(u)_x = \varepsilon u_{xx} + \varepsilon^2 \tau u_{xxt}$
2. Thin film epitaxy: $u_t = (u_x^3)_x - u_{xx} - \delta u_{xxxx}$
3. Phase separation: $u_t = (u^3)_{xx} - u_{xx} - \delta u_{xxxx}$

Cool, Bartol, Kasenga, et al, *Calphad*, 2010

Nonlinear Differential Equations

In general, we can write the equations as

$$u_t = \mathcal{N}u + \mathcal{L}u$$

- u is the variable of interest
- $\mathcal{N}$ is a nonlinear differential operator
- $\mathcal{L}$ is a linear differential operator

Potential numerical difficulties:

- high-order/mixed derivative terms present in the linear operator $\mathcal{L}$
- strong nonlinearity is embedded in operator $\mathcal{N}$
- numerical efficiency: to achieve a desirable resolution

Operator Splitting Methods

$$u_t = \mathcal{N}u + \mathcal{L}u$$

Decompose the full complex equation into two simpler sub-equations

- linear part

$$u_t = \mathcal{L}u \qquad u(x, t+\Delta t) = \mathcal{S}_{\mathcal{L}}(\Delta t)\ u(x,t)$$

- nonlinear part

$$u_t = \mathcal{N}u \qquad u(x, t+\Delta t) = \mathcal{S}_{\mathcal{N}}(\Delta t)\ u(x,t)$$

- $\mathcal{S}_{\mathcal{L}}$ and $\mathcal{S}_{\mathcal{N}}$ are exact solution operators of the equations
- Strang splitting: $\Delta t-$splitting step size

$$u(x, t+\Delta t) = \mathcal{S}_{\mathcal{N}}\left(\frac{\Delta t}{2}\right)\mathcal{S}_{\mathcal{L}}\left(\Delta t\right)\mathcal{S}_{\mathcal{N}}\left(\frac{\Delta t}{2}\right)u(x,t) + \mathcal{O}((\Delta t)^3)$$

- Numerical approximations of $\mathcal{S}_{\mathcal{L}}$ and $\mathcal{S}_{\mathcal{N}}$ separatively $\Rightarrow$ flexibility

Operator Splitting Methods

$$u_t = \mathcal{N}u + \mathcal{L}u$$

Decompose the full complex equation into two simpler sub-equations

- linear part

$$u_t = \mathcal{L}u \qquad u(x, t+\Delta t) = \mathcal{S}_{\mathcal{L}}(\Delta t)\ u(x,t)$$

- nonlinear part

$$u_t = \mathcal{N}u \qquad u(x, t+\Delta t) = \mathcal{S}_{\mathcal{N}}(\Delta t)\ u(x,t)$$

- $\mathcal{S}_{\mathcal{L}}$ and $\mathcal{S}_{\mathcal{N}}$ are exact solution operators of the equations
- Strang splitting: $\Delta t-$splitting step size

$$u(x, t+\Delta t) = \mathcal{S}_{\mathcal{N}}\left(\frac{\Delta t}{2}\right)\mathcal{S}_{\mathcal{L}}\left(\Delta t\right)\mathcal{S}_{\mathcal{N}}\left(\frac{\Delta t}{2}\right)u(x,t) + \mathcal{O}((\Delta t)^3)$$

- Numerical approximations of $\mathcal{S}_{\mathcal{L}}$ and $\mathcal{S}_{\mathcal{N}}$ separatively $\Rightarrow$ flexibility

Convection-Diffusion Equation

Operation splitting technique has been successfully applied on

$$u_t + f(u)_x = \varepsilon u_{xx}$$

- $f(u)$ a nonlinear convection flux
- $\varepsilon > 0$ is the diffusion coefficient

Numerical difficulties (especially in the convection-dominated case):

- too much numerical viscosity $\Rightarrow$ solution under-resolved
- dispersive schemes $\Rightarrow$ may cause spurious oscillations

Convection-Diffusion Equation

Operation splitting technique has been successfully applied on

$$u_t + f(u)_x = \varepsilon u_{xx}$$

- $f(u)$ a nonlinear convection flux
- $\varepsilon > 0$ is the diffusion coefficient

Numerical difficulties (especially in the convection-dominated case):

Viscous Burgers Equation

$$f(u) = u^2/2$$

$$u_0(x) = -\tanh(x)$$

Steady state solution

$$u(x) = -\tanh\left(\frac{1}{2\varepsilon}x\right)$$

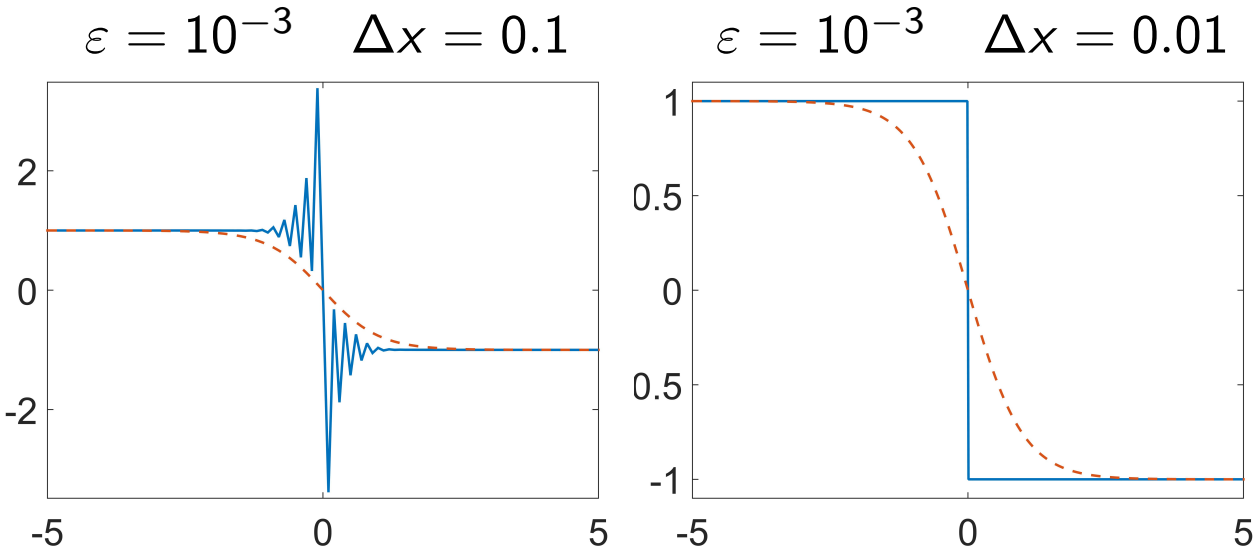

Fast Explicit Operator Splitting (FEOS)

$$u_t + f(u)_x = \varepsilon u_{xx}$$

$u_t + f(u)_x = 0$	Strang splitting	$u_t = \varepsilon u_{xx}$
$\mathcal{S}_{\mathcal{N}}$ nonlinear		$\mathcal{S}_{\mathcal{L}}$ linear

Advantage - flexibility

- $\mathcal{S}_{\mathcal{N}}$ nonlinear: hyperbolic system of conservation law
  1. shock capturing methods
  2. finite-volume method: Godunov-type central-upwind schemes

Fast Explicit Operator Splitting (FEOS)

$$u_t + f(u)_x = \varepsilon u_{xx}$$

$u_t + f(u)_x = 0$	Strang splitting	$u_t = \varepsilon u_{xx}$
$\mathcal{S}_{\mathcal{N}}$ nonlinear		$\mathcal{S}_{\mathcal{L}}$ linear

Advantage - flexibility

- $\mathcal{S}_{\mathcal{L}}$ linear:
  1. method-of-line technique with appropriate ODE solvers
  2. heat kernel
  3. pseudo-spectral framework (FFT algorithm)

  $\Rightarrow$ no enforced stability restriction

Chertock, Kurganov, *Quaderni di Matematica*, 2009

Goal

- to design highly accurate and efficient methods for nonlinear PDEs that arise in various physical phenomena *based on the operator splitting strategy*

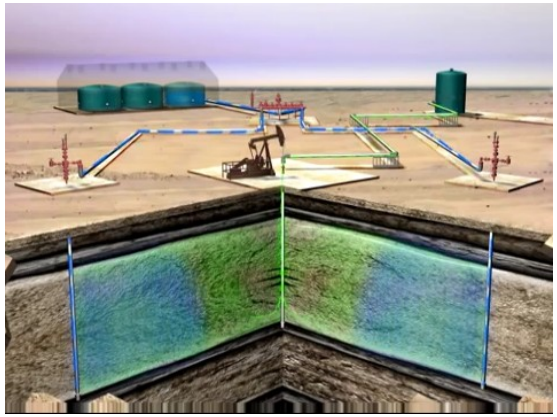

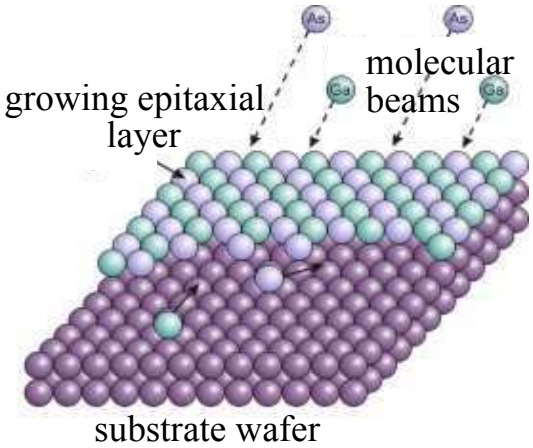

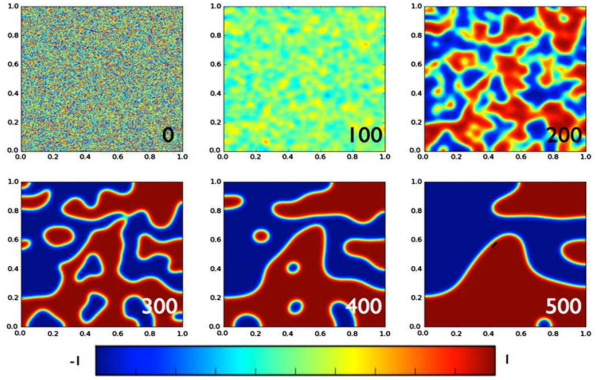

Outlines

Modified Buckley-Leverett (MBL) equation

Physical background - two-phase fluid flow in porous media

Primary Recovery Stage

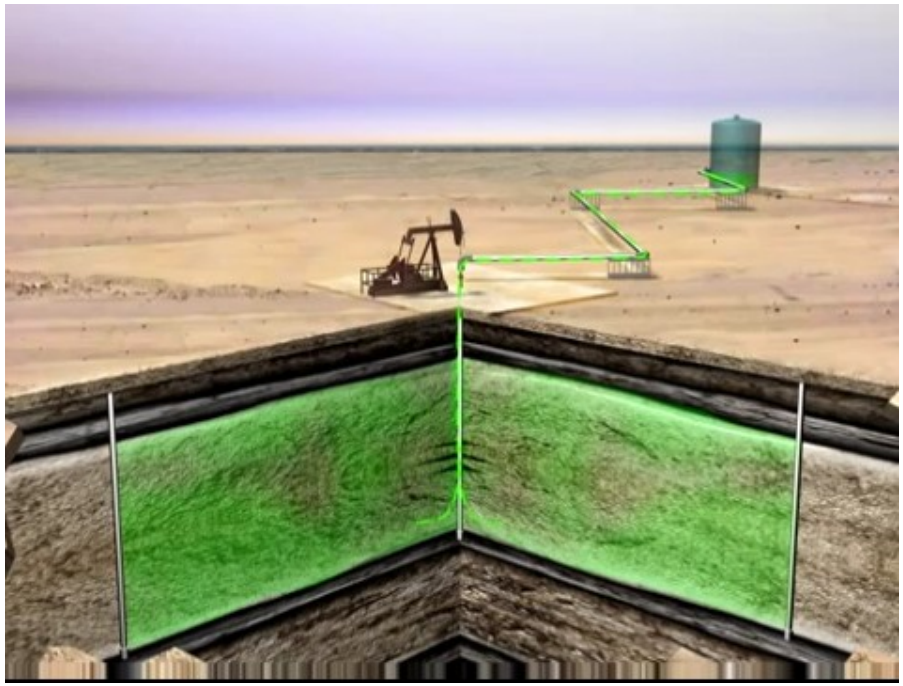

Secondary Recovery Stage

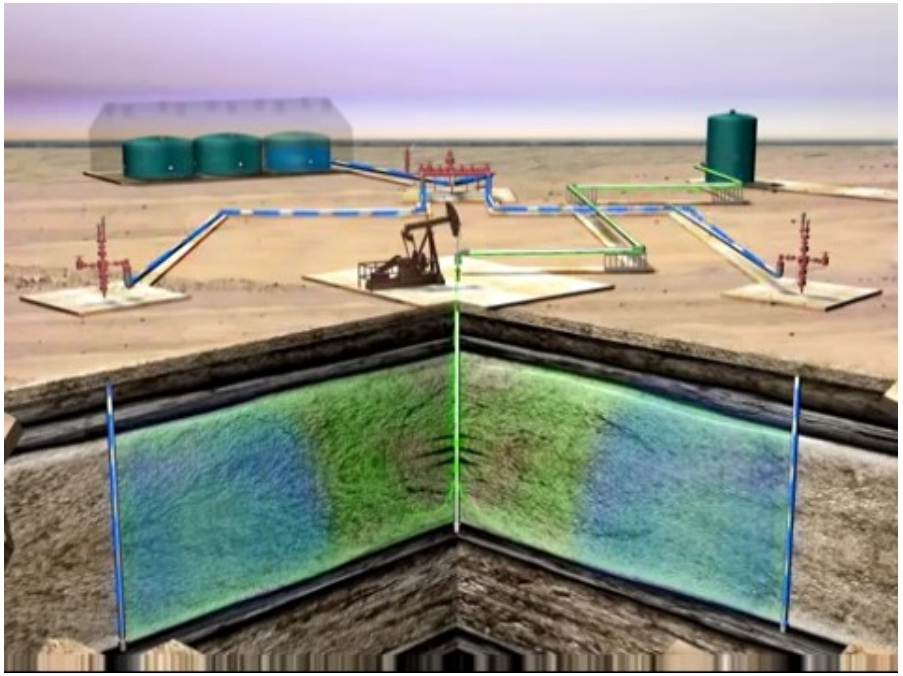

Classical BL $\Rightarrow$ Modified BL

- classical BL equation

$$u_t + f(u)_x = 0$$

$$f(u) = \frac{u^2}{u^2 + M(1-u)^2}$$

- u: water saturation $(0 \le u \le 1)$
- M: viscosity ratio between fluids

Monotone solution for the Riemann Problem

- physical experiments

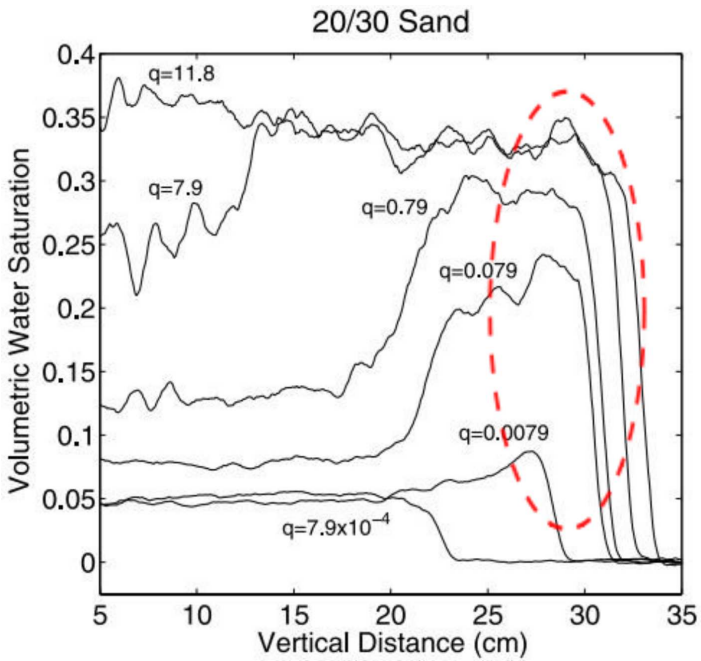

- nonmonotone overshoots

$\Rightarrow$ Modified Buckley-Leverett (MBL) equation

Classical BL $\Rightarrow$ Modified BL

- classical BL equation

$$u_t + f(u)_x = 0$$

$$f(u) = \frac{u^2}{u^2 + M(1-u)^2}$$

- u: water saturation $(0 \le u \le 1)$
- M: viscosity ratio between fluids

Monotone solution for the Riemann Problem

- physical experiments

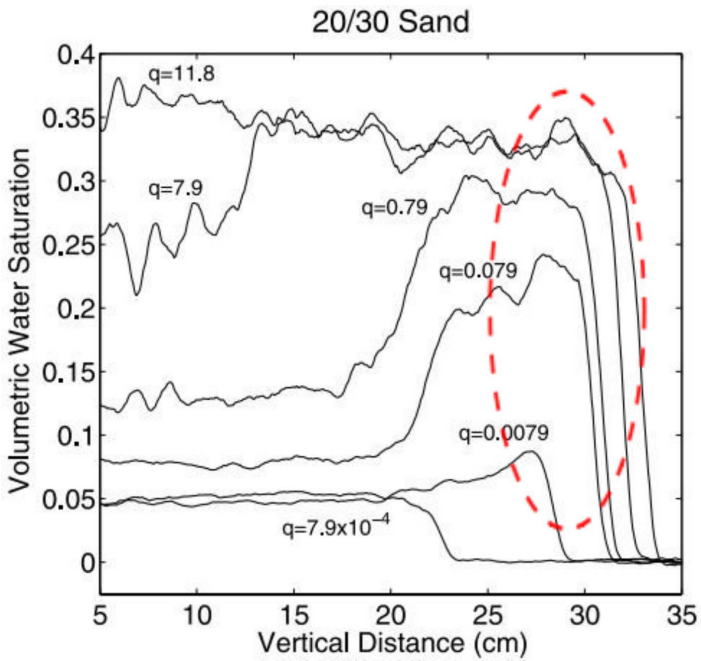

- nonmonotone overshoots

$\Rightarrow$ Modified Buckley-Leverett (MBL) equation

Modified Buckley-Leverett (MBL) equation

- 1-D equation

$$u_t + f(u)_x = \varepsilon u_{xx} + \varepsilon^2 \tau u_{xxt}$$

$$f(u) = \frac{u^2}{u^2 + M(1-u)^2}, \quad \varepsilon > 0,\ \tau > 0$$

- u: water saturation $(0 \le u \le 1)$
- M: viscosity ratio between water and oil

- 2-D equation (with the influence of gravity)

$$u_t + f(u)_x + g(u)_z = \varepsilon \Delta u + \varepsilon^2 \tau \Delta u_t$$

$$g(u) = f(u)(1 - C(1-u)^2), \quad C > 0$$

van Duijn, Peletier, Pop, *SIMA*, 2007 Kao, Kurganov, Qu, Wang, *JSC*, 2015

Modified Buckley-Leverett (MBL) equation

- 1-D equation

$$u_t + f(u)_x = \varepsilon u_{xx} + \varepsilon^2 \tau u_{xxt}$$

$$f(u) = \frac{u^2}{u^2 + M(1-u)^2}, \quad \varepsilon > 0,\ \tau > 0$$

- u: water saturation $(0 \le u \le 1)$
- M: viscosity ratio between water and oil

- 2-D equation (with the influence of gravity)

$$u_t + f(u)_x + g(u)_z = \varepsilon \Delta u + \varepsilon^2 \tau \Delta u_t$$

$$g(u) = f(u)(1 - C(1-u)^2), \quad C > 0$$

van Duijn, Peletier, Pop, *SIMA*, 2007 Kao, Kurganov, Qu, Wang, *JSC*, 2015

Numerical Challenges

$$u_t + f(u)_x = \varepsilon u_{xx} + \varepsilon^2 \tau u_{xxt} \quad f(u) = \frac{u^2}{u^2 + M(1-u)^2}$$

1. nonconvex flux $f(u)$

Numerical Challenges

$$u_t + f(u)_x = \varepsilon u_{xx} + \varepsilon^2 \tau u_{xxt} \quad f(u) = \frac{u^2}{u^2 + M(1-u)^2}$$

1. nonconvex flux $f(u)$

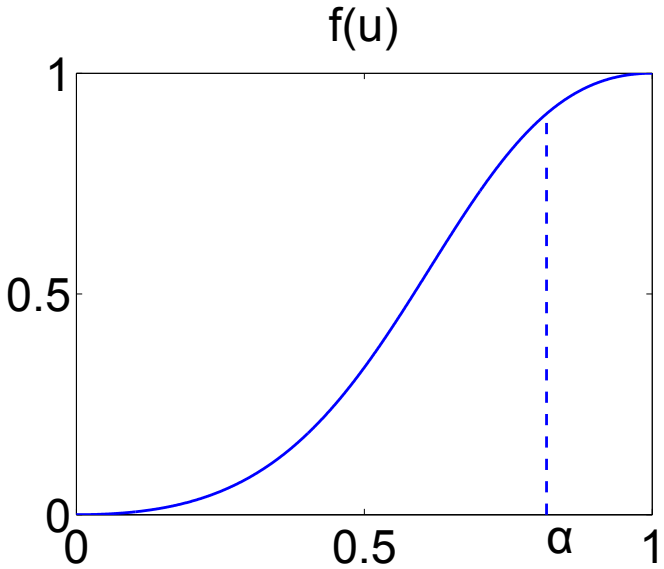

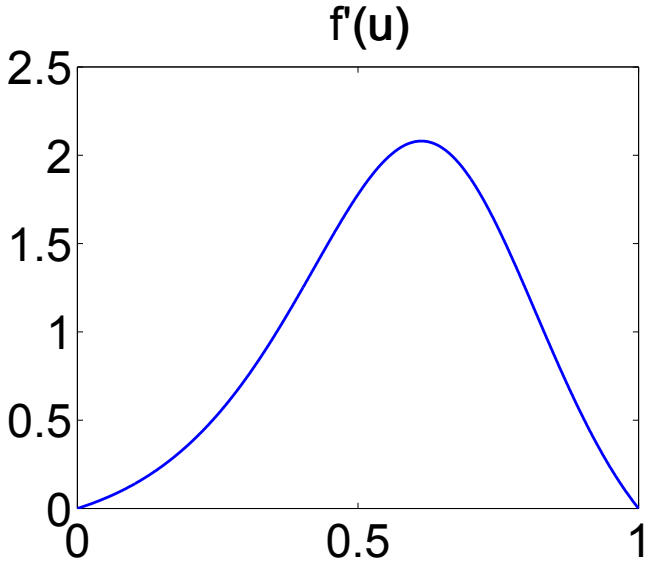

- Solution computed by high-order methods may fail to converge to the entropy solution [Kurganov, Petrova, Popov, *SISC*, 2007]

Numerical Challenges

$$u_t + f(u)_x = \varepsilon u_{xx} + \varepsilon^2 \tau u_{xxt} \quad f(u) = \frac{u^2}{u^2 + M(1-u)^2}$$

1. nonconvex flux $f(u)$
2. high-order terms on the right-hand side

- explicit methods may be inefficient
- especially when a fine mesh is used to accurately capture small scale details of the solution

Numerical Challenges

$$u_t + f(u)_x = \varepsilon u_{xx} + \varepsilon^2 \tau u_{xxt} \quad f(u) = \frac{u^2}{u^2 + M(1-u)^2}$$

1. nonconvex flux $f(u)$
2. high-order terms on the right-hand side

- van Duijn, Peletier, Pop, *SIMA*, 2007
  - first order finite difference scheme with Forward Euler
  - solve a linear system for each time step ($\varepsilon^2 \tau u_{xxt}$)
- Wang, Kao, *JCS*, 2013
  - second- and third-order semi-discrete central scheme
  - high order ODE solver (Runge-Kutta methods)

Numerical Challenges

$$u_t + f(u)_x = \varepsilon u_{xx} + \varepsilon^2 \tau u_{xxt} \quad f(u) = \frac{u^2}{u^2 + M(1-u)^2}$$

1. nonconvex flux $f(u)$
2. high-order terms on the right-hand side

- van Duijn, Peletier, Pop, *SIMA*, 2007
  - first order finite difference scheme with Forward Euler
  - solve a linear system for each time step ($\varepsilon^2 \tau u_{xxt}$)
- Wang, Kao, *JCS*, 2013
  - second- and third-order semi-discrete central scheme
  - high order ODE solver (Runge-Kutta methods)

Goal

- develop a highly accurate and efficient method
- extend it to a more numerically demanding 2-D case

Fast Operator Splitting Methods for MBL

$$u_t + f(u)_x = \varepsilon u_{xx} + \varepsilon^2 \tau u_{xxt}$$

$$(u - \varepsilon^2 \tau u_{xx})_t + f(u)_x = \varepsilon u_{xx}$$

$$(u - \varepsilon^2 \tau u_{xx})_t + f(u)_x = 0$$

$\mathcal{S}_{\mathcal{N}}$ nonlinear part

Strang splitting

$$(u - \varepsilon^2 \tau u_{xx})_t = \varepsilon u_{xx}$$

$\mathcal{S}_{\mathcal{L}}$ linear part

- Second-order Strang splitting

$$u(x, t + \Delta t) \approx \mathcal{S}_{\mathcal{N}}\left(\frac{\Delta t}{2}\right) \mathcal{S}_{\mathcal{L}}(\Delta t)\, \mathcal{S}_{\mathcal{N}}\left(\frac{\Delta t}{2}\right) u(x, t)$$

Nonlinear part ($\mathcal{S}_{\mathcal{N}}$) $\quad (u - \varepsilon^2 \tau u_{xx})_t + f(u)_x = 0$

1. introduce an intermediate variable v: $\begin{aligned} v_t + f(u)_x &= 0 \\ u - \varepsilon^2 \tau u_{xx} &= v \end{aligned}$
2. finite volume method on v: semi-discrete central-upwind scheme [Kurganov, Petrova, Popov, *SISC*, 2007]

Nonlinear part ($\mathcal{S}_{\mathcal{N}}$) $\quad (u - \varepsilon^2 \tau u_{xx})_t + f(u)_x = 0$

1. introduce an intermediate variable v: $\begin{aligned} v_t + f(u)_x &= 0 \\ u - \varepsilon^2 \tau u_{xx} &= v \end{aligned}$
2. finite volume method on v: semi-discrete central-upwind scheme [Kurganov, Petrova, Popov, *SISC*, 2007]

The formal spatial order of the scheme = the formal order of the reconstruction.

- second-order: generalized minmod-based reconstruction [van Leer, *JCP*, 1979]

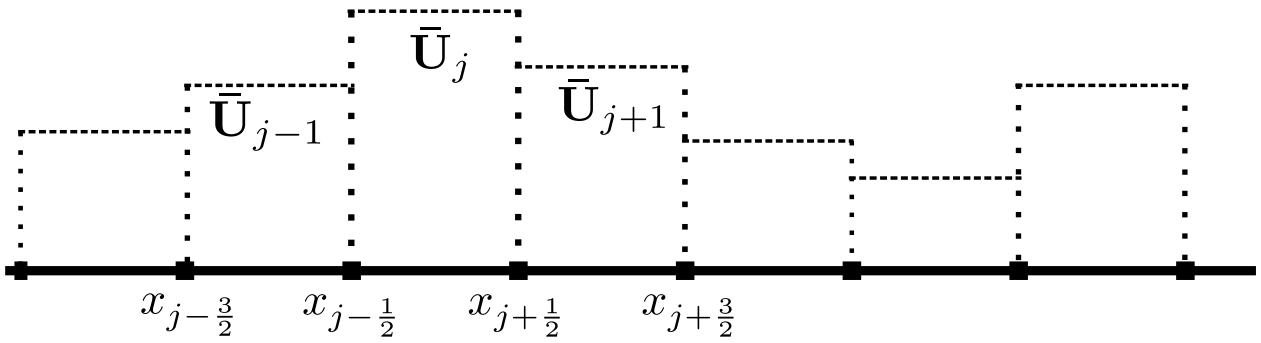

Nonlinear part ($\mathcal{S}_{\mathcal{N}}$) $\quad (u - \varepsilon^2 \tau u_{xx})_t + f(u)_x = 0$

1. introduce an intermediate variable v: $\begin{aligned} v_t + f(u)_x &= 0 \\ u - \varepsilon^2 \tau u_{xx} &= v \end{aligned}$
2. finite volume method on v: semi-discrete central-upwind scheme [Kurganov, Petrova, Popov, *SISC*, 2007]

The formal spatial order of the scheme = the formal order of the reconstruction.

- second-order: generalized minmod-based reconstruction [van Leer, *JCP*, 1979]

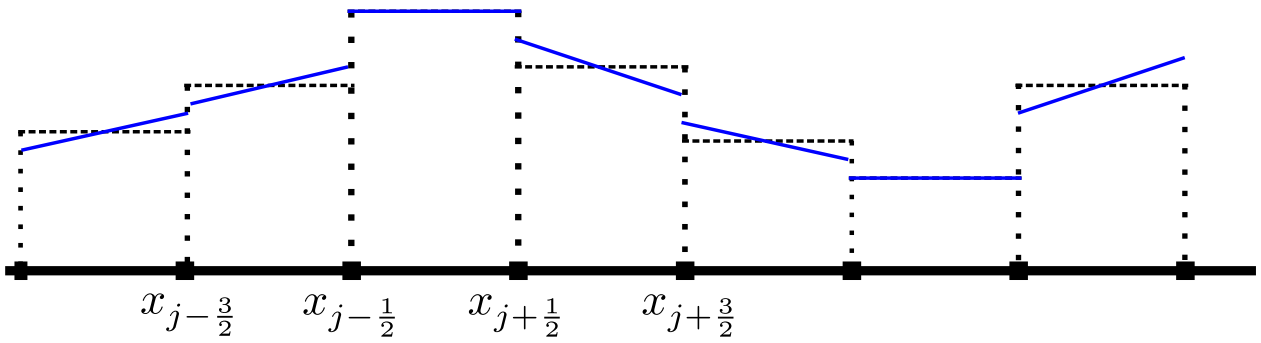

Nonlinear part ($\mathcal{S}_{\mathcal{N}}$) $\quad (u - \varepsilon^2 \tau u_{xx})_t + f(u)_x = 0$

1. introduce an intermediate variable v: $\begin{aligned} v_t + f(u)_x &= 0 \\ u - \varepsilon^2 \tau u_{xx} &= v \end{aligned}$
2. finite volume method on v: semi-discrete central-upwind scheme [Kurganov, Petrova, Popov, *SISC*, 2007]

The formal spatial order of the scheme = the formal order of the reconstruction.

- second-order: generalized minmod-based reconstruction [van Leer, *JCP*, 1979]

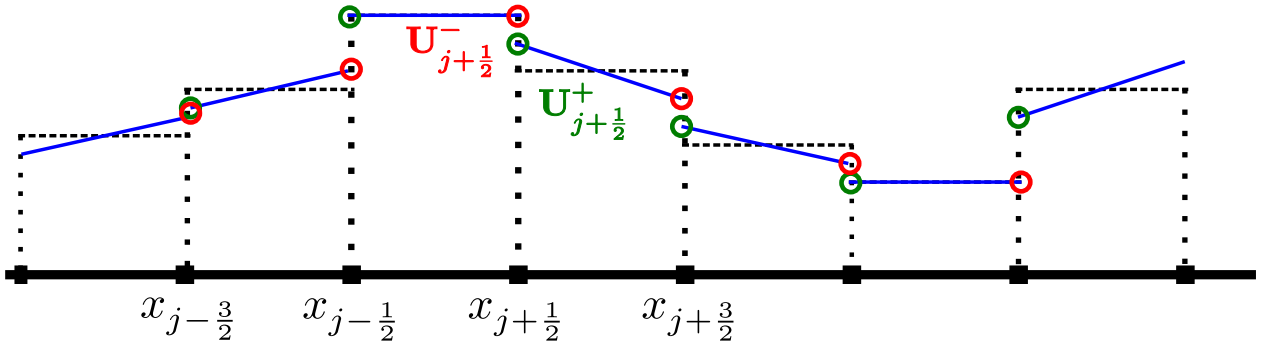

Nonlinear part ($\mathcal{S}_{\mathcal{N}}$) $\quad (u - \varepsilon^2 \tau u_{xx})_t + f(u)_x = 0$

1. introduce an intermediate variable v: $\begin{aligned} v_t + f(u)_x &= 0 \\ u - \varepsilon^2 \tau u_{xx} &= v \end{aligned}$
2. finite volume method on v: semi-discrete central-upwind scheme [Kurganov, Petrova, Popov, *SISC*, 2007]

The formal spatial order of the scheme = the formal order of the reconstruction.

- second-order: generalized minmod-based reconstruction [van Leer, *JCP*, 1979]
- fifth-order: WENO5 approach [Shu, *Springer*; 1998]

Nonlinear part ($\mathcal{S}_{\mathcal{N}}$) $\quad (u - \varepsilon^2 \tau u_{xx})_t + f(u)_x = 0$

1. introduce an intermediate variable v: $\begin{aligned} v_t + f(u)_x &= 0 \\ u - \varepsilon^2 \tau u_{xx} &= v \end{aligned}$
2. finite volume method on v: semi-discrete central-upwind scheme [Kurganov, Petrova, Popov, *SISC*, 2007]
3. third-order strong stability preserving Runge-Kutta method [Shu, *SISC*, 1988]
4. recover u from v: pseudo-spectral method

$$u(x) = \sum_m \widehat{u}_m e^{imx} \qquad v(x) = \sum_m \widehat{v}_m e^{imx}$$

$$\widehat{u}_m = \frac{\widehat{v}_m}{1 + \varepsilon^2 \tau m^2}$$

Linear part ($\mathcal{S}_{\mathcal{L}}$) $\quad (u - \varepsilon^2 \tau u_{xx})_t = \varepsilon u_{xx}$

- pseudo-spectral method $\quad u(x,t) = \sum_m \widehat{u}_m(t)\, e^{imx}$

$$\frac{d}{dt}\left[\widehat{u}_m(t) - \varepsilon^2 \tau (im)^2 \widehat{u}_m\right] = \varepsilon (im)^2 \widehat{u}_m$$

solve exactly on the time interval $(t, t+\Delta t]$ for any Δt:

$$\widehat{u}_m(t+\Delta t) = \exp\left(\frac{-\varepsilon m^2 \Delta t}{1+\varepsilon^2 \tau m^2}\right) \widehat{u}_m(t)$$

- Fast Fourier Transform (FFT) algorithm

$$\widehat{u}_m \Leftrightarrow u_m$$

EX1 – Accuracy Test on Linear Problem ($\varepsilon = 10^{-3}$)

- 1-D case $\begin{cases} u_t + u_x = \varepsilon u_{xx} + 5\varepsilon^2 u_{xxt}, & (x,t) \in (0,2) \times (0,2], \\ u(x,0) = \sin(\pi x), & x \in [0,2]. \end{cases}$

1. minmod-based reconstruction (second order)

N	L_1 error	rate	L_2 error	rate	L_∞ error	rate
64	1.4755E-02	-	1.3400E-02	-	2.4467E-02	-
128	2.6529E-03	2.4755	2.4454E-03	2.4541	5.9092E-03	2.0498
256	4.5606E-04	2.5403	3.7676E-04	2.6983	9.7694E-04	2.5966
512	1.0240E-04	2.1551	8.0050E-05	2.2347	1.1068E-04	3.1418
1024	2.5122E-05	2.0272	1.9691E-05	2.0233	1.9653E-05	2.4936
2048	6.2732E-06	2.0017	4.9248E-06	1.9994	4.9236E-06	1.9969

2. WENO5 reconstruction (fifth order $\rightarrow$ third order – ODE solver)

N	L_1 error	rate	L_2 error	rate	L_∞ error	rate
64	1.3145E-05	-	1.0293E-05	-	1.0782E-05	-
128	8.6308E-07	3.9289	6.7674E-07	3.9269	6.7037E-07	4.0076
256	8.3592E-08	3.3681	6.5634E-08	3.3661	6.4986E-08	3.3667
512	9.6942E-09	3.1082	7.6128E-09	3.1079	7.5732E-09	3.1012
1024	1.1924E-09	3.0233	9.3638E-10	3.0233	9.3454E-10	3.0186
2048	1.5306E-10	2.9617	1.2021E-10	2.9616	1.2057E-10	2.9544

Example 1 – Accuracy Test on Linear Problem ($\varepsilon = 10^{-3}$)

- 2-D case

$$\begin{cases} u_t + u_x + u_y = \varepsilon \Delta u + 5\varepsilon^2 (\Delta u)_t, & (x,y) \in (0,2) \times (0,2), \ t \in (0,2], \\ u(x,y,0) = \sin(\pi x) + \sin(\pi y), & (x,y) \in (0,2) \times (0,2), \end{cases}$$

2. WENO5 reconstruction (fifth order $\rightarrow$ third order – ODE solver)

N	L_1 error	rate	L_2 error	rate	L_∞ error	rate
64×64	3.3396E-05	-	2.0586E-05	-	2.1565E-05	-
128×128	2.1915E-06	3.9297	1.3535E-06	3.9269	1.3407E-06	4.0076
256×256	2.1273E-07	3.3648	1.3127E-07	3.3661	1.2997E-07	3.3667
512×512	2.4679E-08	3.1077	1.5226E-08	3.1079	1.5146E-08	3.1012
1024×1024	3.0370E-09	3.0226	1.8736E-09	3.0226	1.8690E-09	3.0185

Example 2 – Accuracy Test on Nonlinear Problem

$$\begin{cases} u_t + f(u)_x = \varepsilon u_{xx} + 0.2\varepsilon^2 u_{xxt}, & (x,t) \in (0,2) \times (0, 0.125], \\ u(x,0) = 0.45(\sin(\pi x) + 1), & x \in [0,2]. \end{cases}$$

1. minmod-based reconstruction

N	L_1 error	rate	L_2 error	rate	L_∞ error	rate
64	5.1709E-03	-	1.1041E-02	-	4.9341E-02	-
128	1.7538E-03	1.5600	5.1379E-03	1.1036	3.5078E-02	0.4922
256	5.3929E-04	1.7013	1.9756E-03	1.3789	1.8171E-02	0.9490
512	1.4631E-04	1.8821	6.1700E-04	1.6790	6.7943E-03	1.4192
1024	3.6482E-05	2.0038	1.6260E-04	1.9239	2.0300E-03	1.7429
2048	8.8589E-06	2.0420	3.9584E-05	2.0383	5.0771E-04	1.9994

2. WENO5 reconstruction (slightly higher than minmod)

N	L_1 error	rate	L_2 error	rate	L_∞ error	rate
64	2.8837E-03	-	7.5782E-03	-	4.0485E-02	-
128	8.6877E-04	1.7309	3.1722E-03	1.2564	2.2508E-02	0.8469
256	2.0925E-04	2.0538	9.6753E-04	1.7131	8.8667E-03	1.3440
512	3.9587E-05	2.4021	1.9185E-04	2.3344	2.0925E-03	2.0832
1024	7.7174E-06	2.3588	3.1650E-05	2.5997	3.5922E-04	2.5422
2048	1.7354E-06	2.1529	6.5627E-06	2.2698	6.8772E-05	2.3850

Example 2 – Accuracy Test on Nonlinear Problem

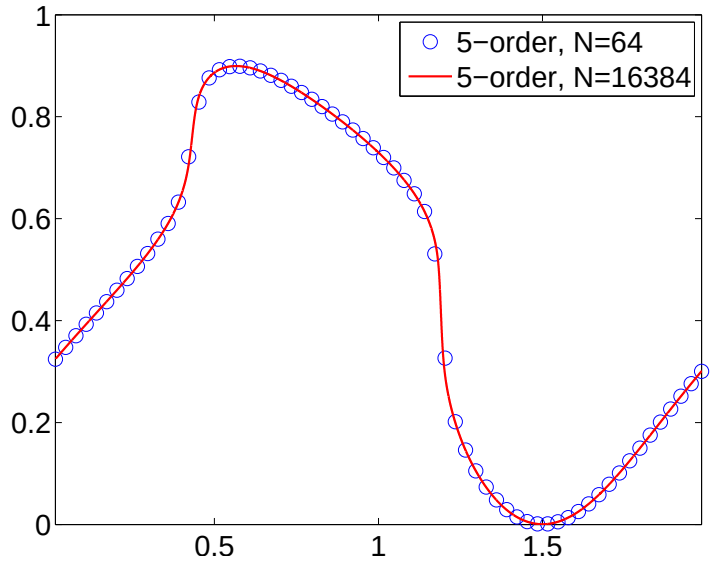

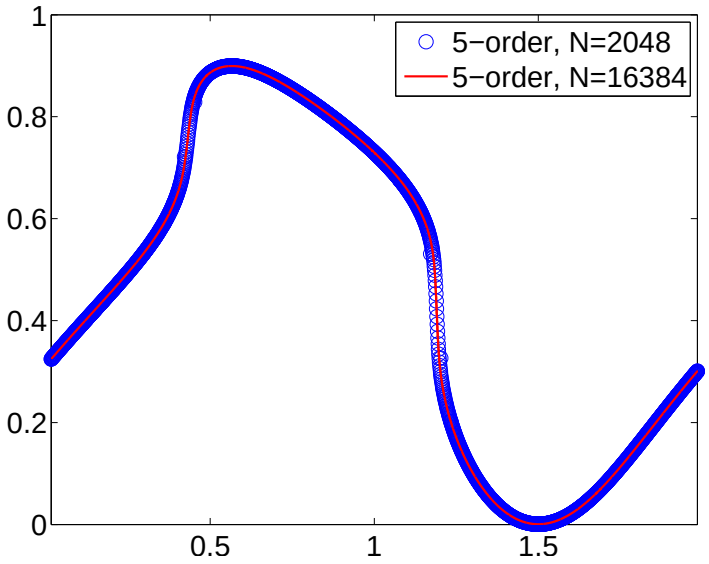

Convergence rates here are lower due to ...

- the nonlinearity in the flux $f \Rightarrow$ sharp gradient areas
- the fifth-order WENO5 reconstruction still leads to slightly higher experimental convergence rates and smaller errors

Example 3 – Riemann Problem [van Duijn, Peletier etc; 2007]

1-D MBL equation with $u(x,0) = \begin{cases} u_B, & \text{if } x \in (0.75, 2.25), \\ 0, & \text{otherwise} \end{cases} \quad x \in [0,3].$

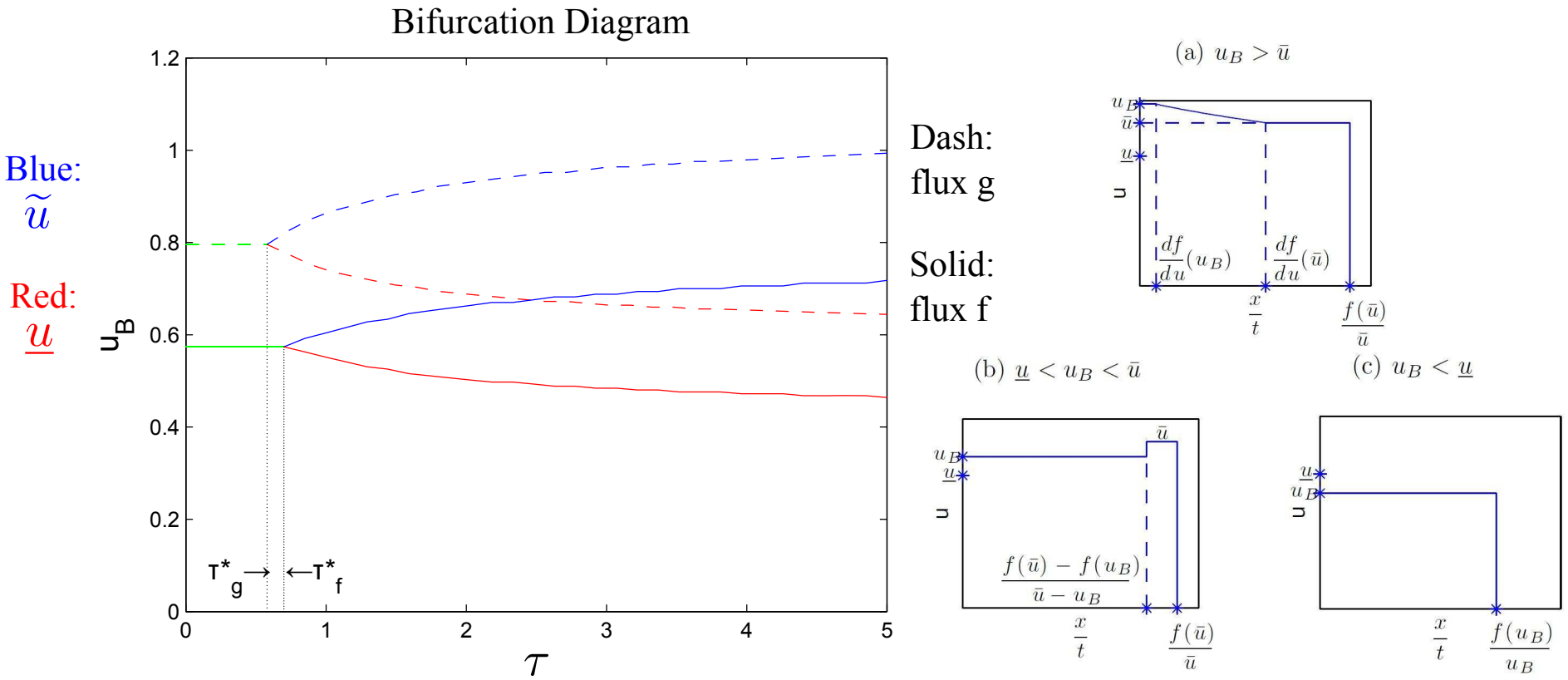

Case 1: $\tau = 3.5$, $u_B = 0.85 > \widetilde{u}$

- By bifurcation diagram: plateau height $\widetilde{u} \approx 0.698$
- Shock location $x \approx 2.893$

(a) $u_B > \bar{u}$

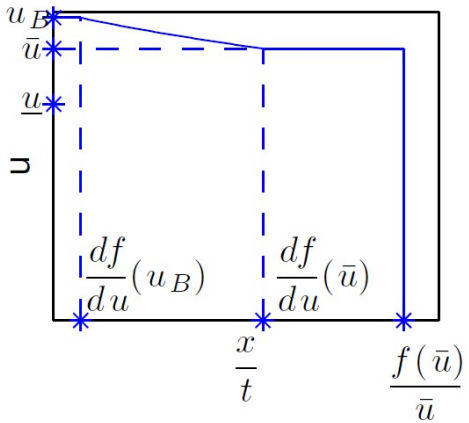

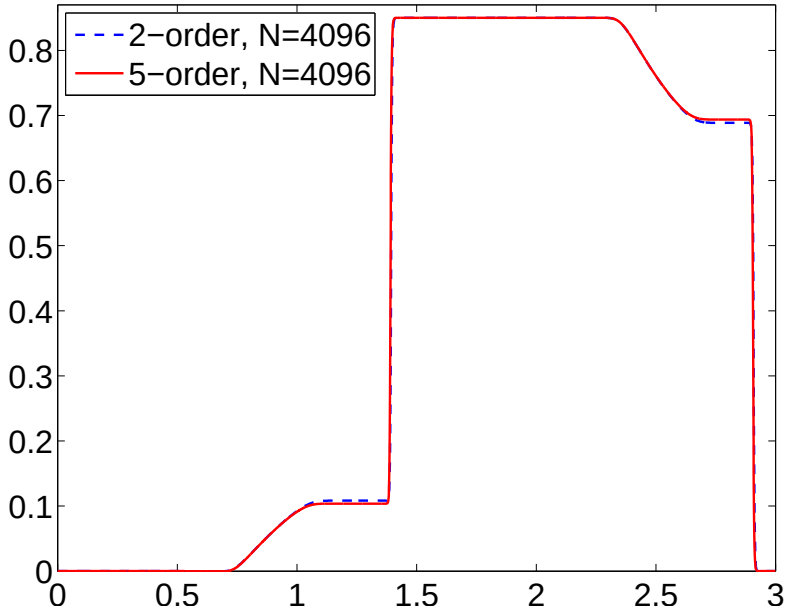

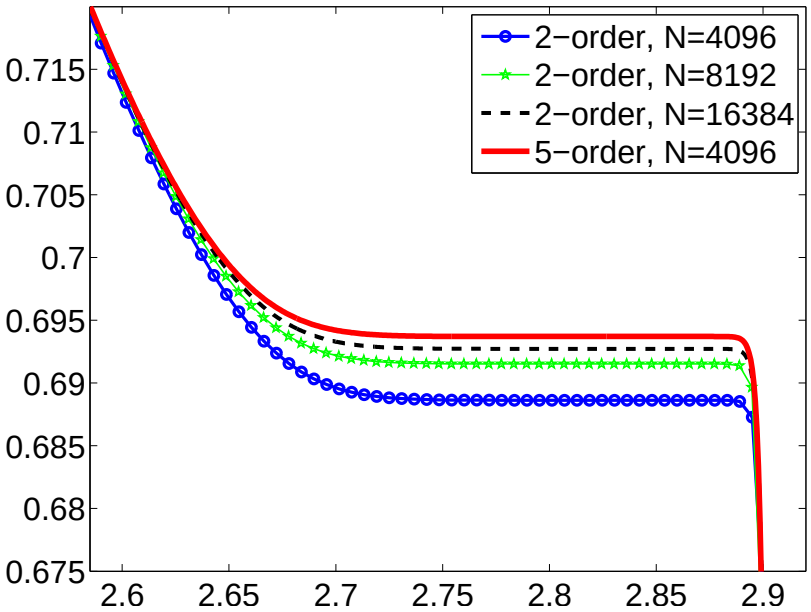

Case 2: $\tau = 5$, $\underline{u} < u_B = 0.66 < \widetilde{u}$

- By bifurcation diagram: plateau height $\widetilde{u} \approx 0.713$
- Jump up at $x \approx 2.597$
- Jump down at $x \approx 2.881$

(b) $\underline{u} < u_B < \bar{u}$

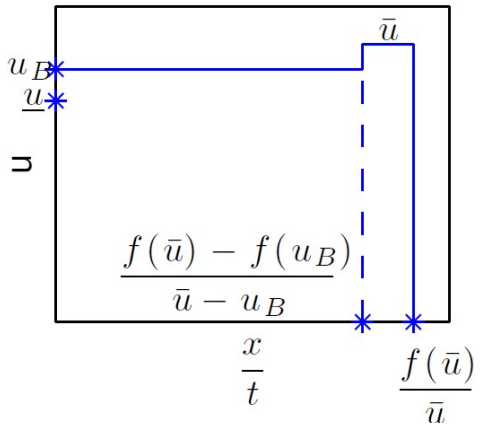

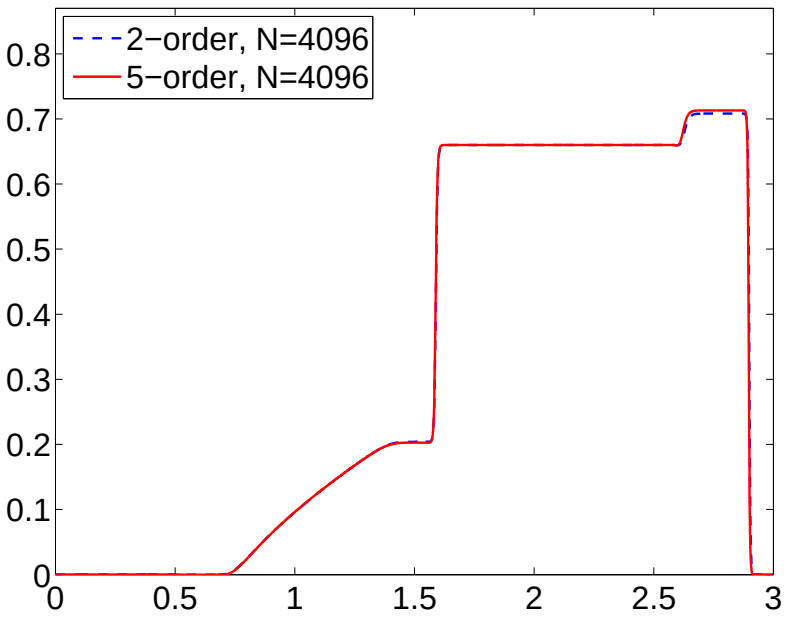

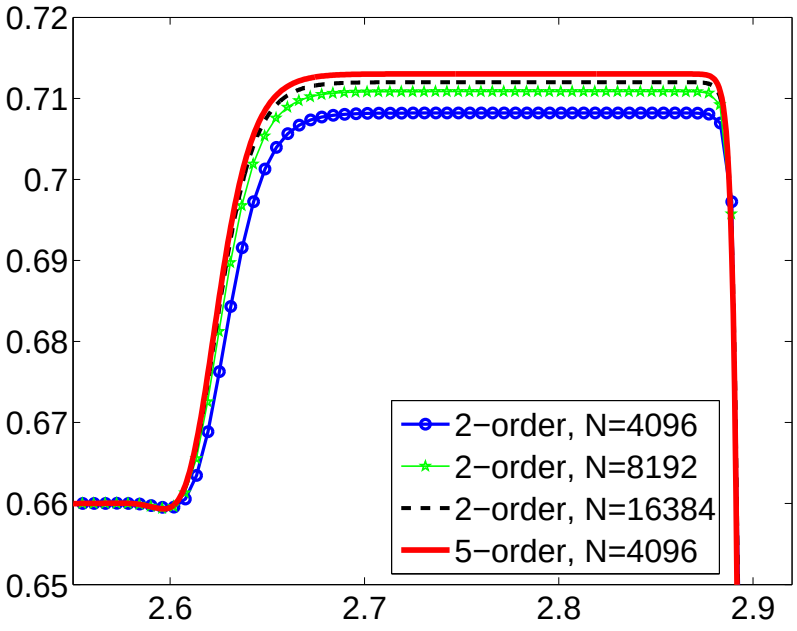

Case 3: $\tau = 5$, $\underline{u} < u_B = 0.52 < \widetilde{u}$

- By bifurcation diagram: plateau height $\widetilde{u} \approx 0.713$
- Physical oscillations around $x \approx 2.8$
- Jump down at $x \approx 2.881$

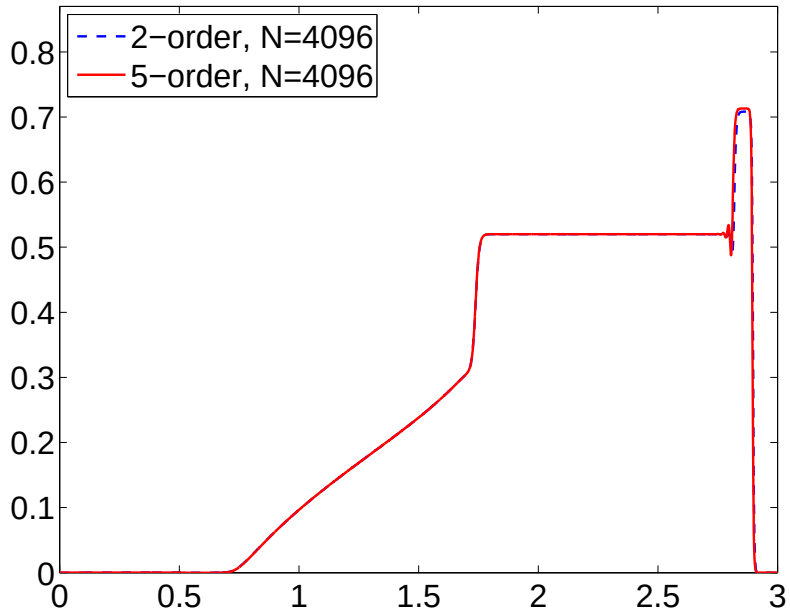

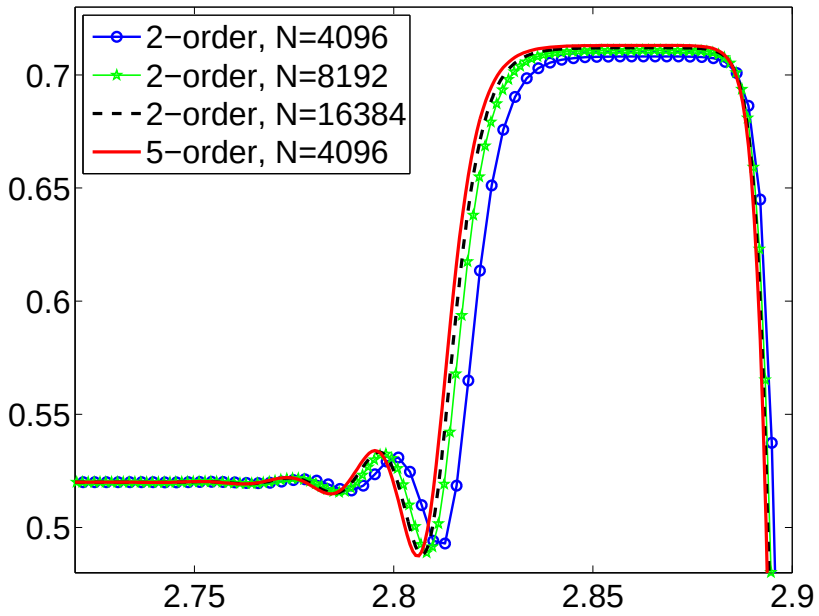

Computational Cost

- To perform a fair comparison between minmod and WENO5

	Example 1		**Example 2**		**Example 3**	
N	minmod	WENO5	minmod	WENO5	minmod	WENO5
1024	1.3572	1.9812	1.3884	2.0124	1.3728	2.0280
2048	5.8656	8.4085	6.3492	8.2525	5.8500	8.4865
4096	25.8494	36.2234	25.8962	35.7398	25.6778	36.0674
8192	112.6483	151.3210	111.6499	151.2274	108.9511	151.9762
16384	476.3802	617.8264	474.6018	630.4156	470.7018	627.5422

- For a fixed grid, computational cost is increased by about 35% for WENO5 approach
- But to achieve comparable solution quality, four times denser grids for minmod

WENO5-based method is more accurate and more efficient.

Example 4 – 2-D BL and MBL Equations (1)

$$BL: u_t + f(u)_x + g(u)_z = 0$$

$$MBL: u_t + f(u)_x + g(u)_z = \varepsilon \Delta u + \varepsilon^2 \tau \Delta u_t$$

where

$$f(u) = \frac{u^2}{u^2 + M(1-u)^2}, \quad g(u) = f(u)(1 - 2(1-u)^2)$$

with initial condition: a smooth two-dimensional Gaussian function

$$u(x, z, 0) = 5e^{-20(x^2+z^2)}$$

cut off by a plateau $u = 0.85$. Here, $M = 1/2, \tau = 2.5, \varepsilon = 10^{-3}$.

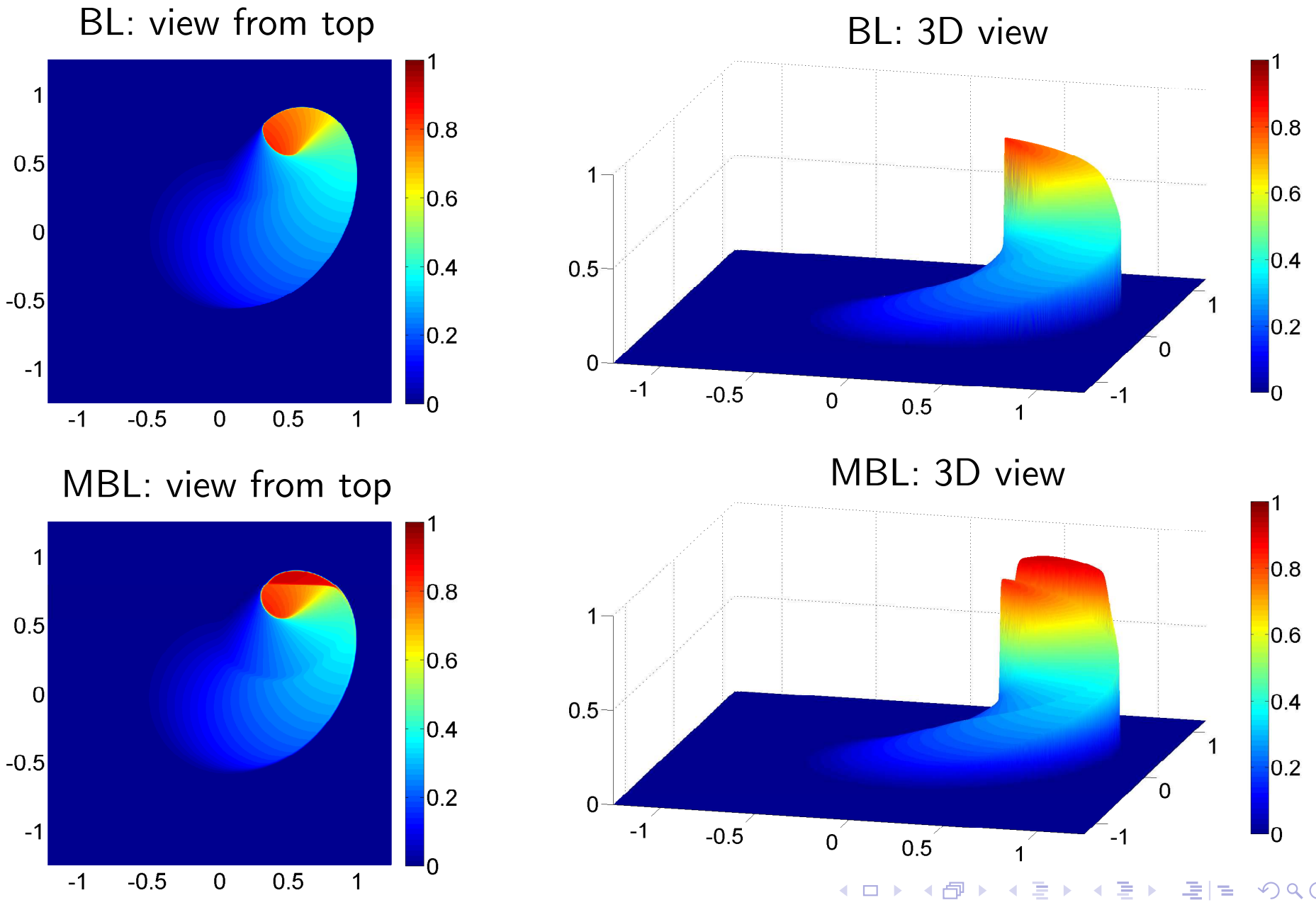
BL: view from top
BL: 3D view
MBL: view from top
MBL: 3D view

Example 5 – 2-D BL and MBL Equations (2)

The second initial condition is a nonsmooth function

$$u(x,z,0) = \begin{cases} u_B, & \text{if } \ 0.75 \le |x| \le 2.25, \quad \text{or} \quad 0.75 \le |z| \le 2.25, \\ 0, & \text{otherwise} \end{cases}$$

in the computational domain $[0,3]^2$ with $\tau = 2.5, M = 1/2$, and $u_B = 0.85$.

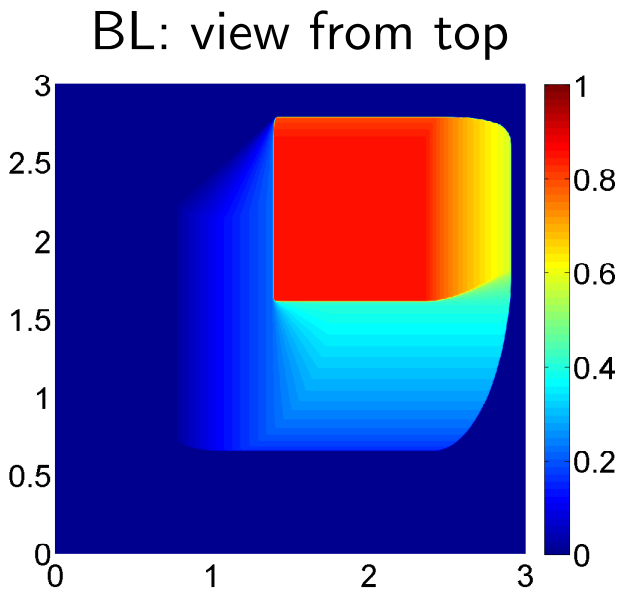
BL: view from top
0
0.5
1
1.5
2
2.5
3
0
1
2
3
0
0.2
0.4
0.6
0.8
1

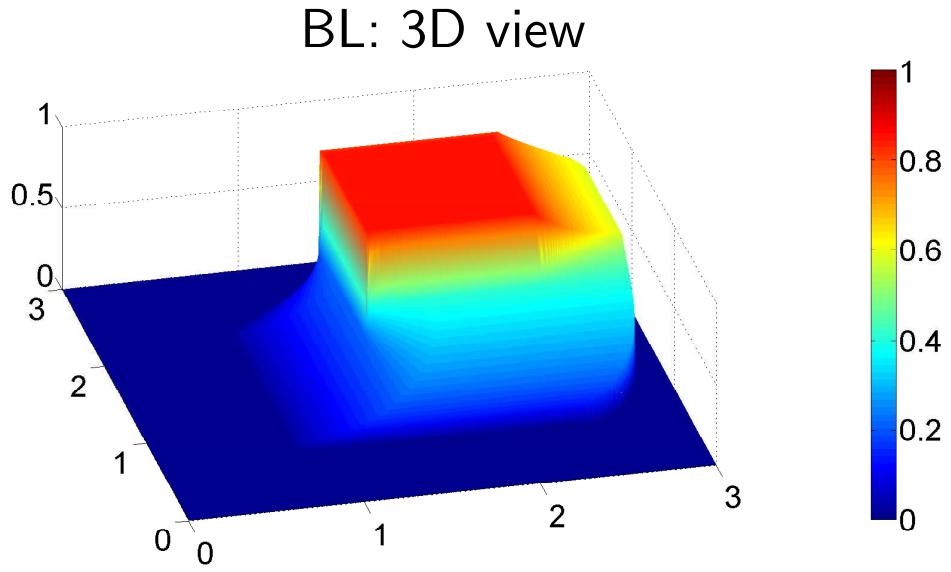
BL: 3D view
0
0.5
1
0
1
2
3
0
1
2
3
0
0.2
0.4
0.6
0.8
1

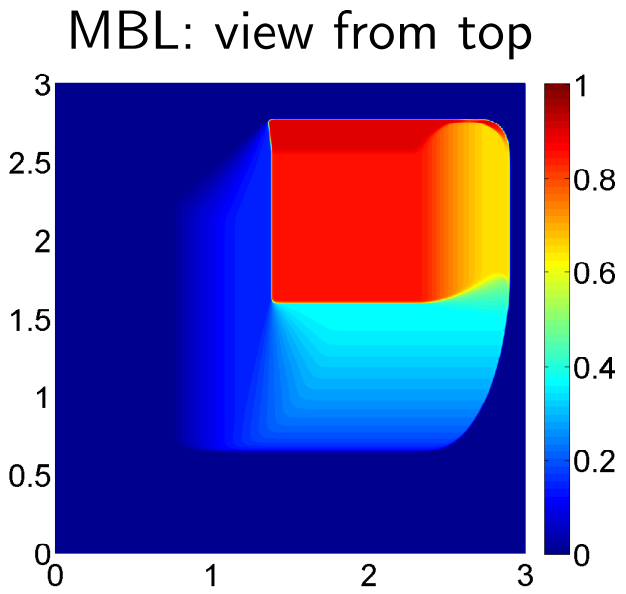
MBL: view from top
0
0.5
1
1.5
2
2.5
3
0
1
2
3
0
0.2
0.4
0.6
0.8
1

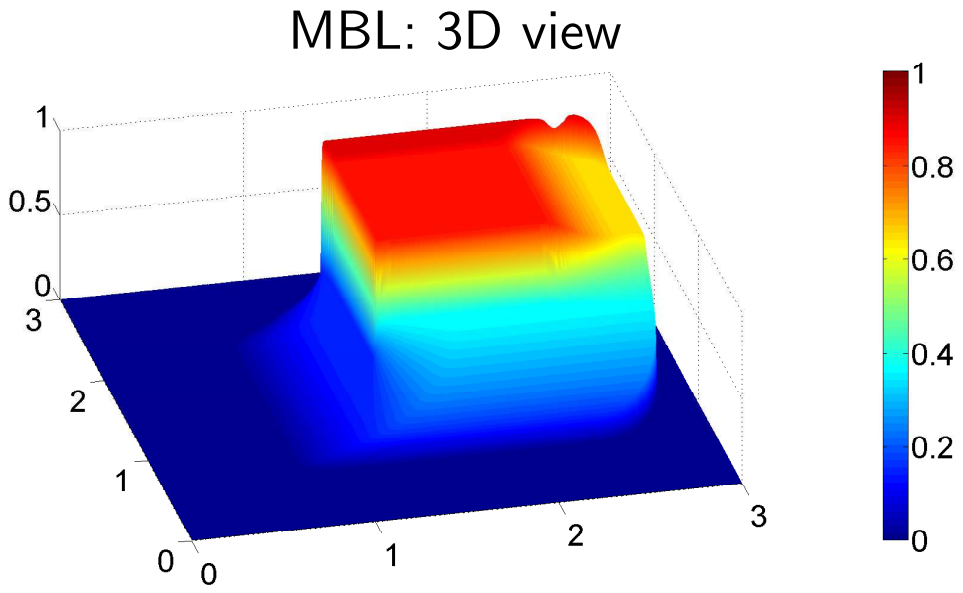
MBL: 3D view
0
0.5
1
0
1
2
3
0
1
2
3
0
0.2
0.4
0.6
0.8
1

Outlines

Phase Field Models: mathematical models for interfacial problems

1. Thin film epitaxy: the deposition of a crystalline overlayer on a crystalline substrate

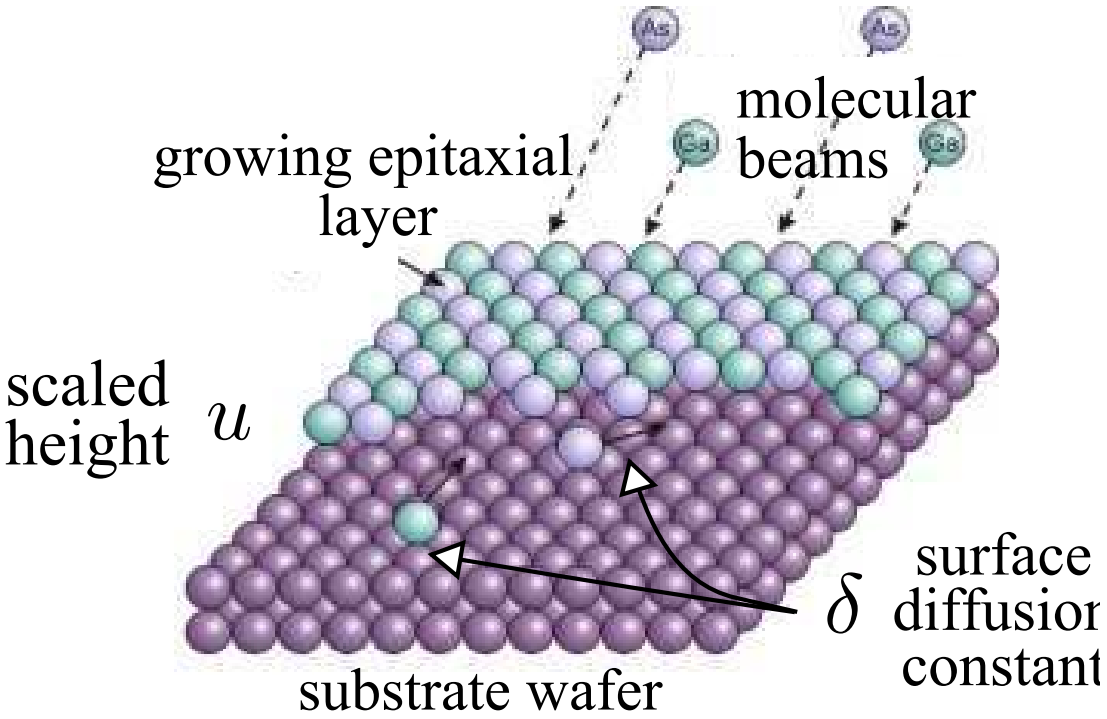

- molecular beam epitaxy (MBE) equation with slope selection

$$u_t = -\delta\Delta^2 u - \nabla\cdot[(1-|\nabla u|^2)\nabla u], \quad \boldsymbol{x}\in\Omega\subset\mathbb{R}^2$$

2. Phase separation: two components of a binary fluid spontaneously separate and form domains pure in each component

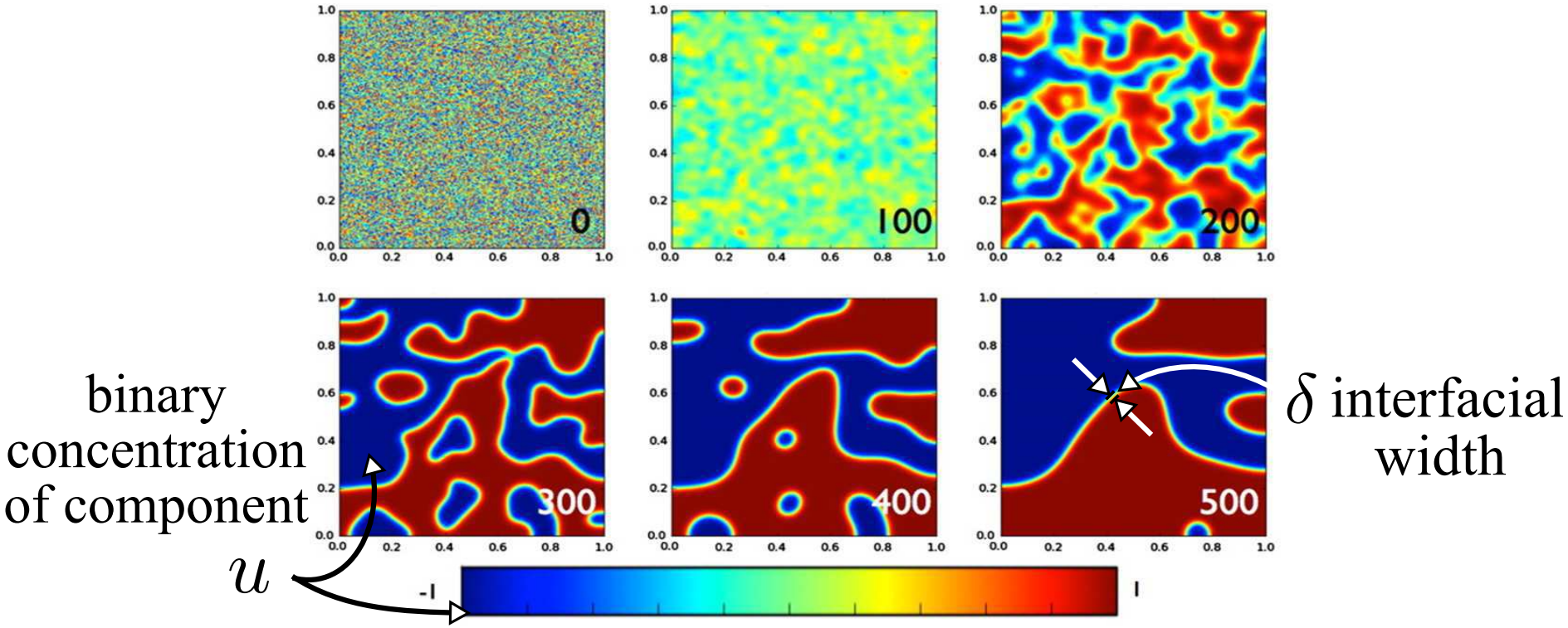

- Cahn-Hilliard (CH) equation:

$$u_t = -\delta\Delta^2 u + \Delta(u^3 - u), \quad \boldsymbol{x} \in \Omega \subset \mathbb{R}^2$$

Energy Functionals

- An important feature of these two equations is that they can be viewed as the gradient flow of energy functionals:

1. MBE $$u_t = -\delta\Delta^2 u - \nabla\cdot[(1-|\nabla u|^2)\nabla u]$$

2. CH $$u_t = -\delta\Delta^2 u + \Delta(u^3 - u)$$

Energy Functionals

- An important feature of these two equations is that they can be viewed as the gradient flow of energy functionals:

1. MBE
$$u_t = -\delta\Delta^2 u - \nabla\cdot[(1-|\nabla u|^2)\nabla u]$$
$$E(u) = \int_\Omega \left[\frac{\delta}{2}|\Delta u|^2 + \frac{1}{4}(|\nabla u|^2 - 1)^2\right] d\boldsymbol{x}$$
2. CH
$$u_t = -\delta\Delta^2 u + \Delta(u^3 - u)$$
$$E(u) = \int_\Omega \left[\frac{\delta}{2}|\nabla u|^2 + \frac{1}{4}(u^2 - 1)^2\right] d\boldsymbol{x}$$

- energy decay property [Cahn, Hillard, *J. Chem. Phys*, 1958] [Li, Liu, *EJAM*, 2003]
$$E\left(u(t)\right) \le E\left(u(s)\right),\ \forall t \ge s$$

Numerical Challenges

$$MBE \quad u_t = -\delta\Delta^2 u - \nabla\cdot[(1-|\nabla u|^2)\nabla u]$$

$$CH \quad u_t = -\delta\Delta^2 u + \Delta(u^3 - u)$$

- severe timestep restriction $\delta\Delta^2(\cdot)$
- phase-field models: long-time simulations to attain steady state
- nonlinear energy stability $\Rightarrow$ nonphysical oscillations.

Numerical Challenges

$$MBE \quad u_t = -\delta\Delta^2 u - \nabla\cdot[(1-|\nabla u|^2)\nabla u]$$

$$CH \quad u_t = -\delta\Delta^2 u + \Delta(u^3 - u)$$

- severe timestep restriction $\delta\Delta^2(\cdot)$
- phase-field models: long-time simulations to attain steady state
- nonlinear energy stability $\Rightarrow$ nonphysical oscillations.

Semi-implicit schemes are widely used

- [*Xu*, *Tang*; 2006][*He*, *Liu*, *Tang*; 2007] include an extra stabilization term
- [*Qiao*, *Zhang*, *Tang*; 2011][*Zhang*, *Qiao*; 2012] unconditional energy stable finite-difference schemes with adaptive time-stepping strategy
- [*Tierra*, *Guillén-González*; 2015] a detailed review of the recent updates on numerical methods for phase-field models

Numerical Challenges

$$MBE \quad u_t = -\delta\Delta^2 u - \nabla\cdot[(1-|\nabla u|^2)\nabla u]$$

$$CH \quad u_t = -\delta\Delta^2 u + \Delta(u^3 - u)$$

- severe timestep restriction $\delta\Delta^2(\cdot)$
- phase-field models: long-time simulations to attain steady state
- nonlinear energy stability $\Rightarrow$ nonphysical oscillations.

Goal

Develop numerical schemes for MBE and CH equations that are

- explicit
- efficient and stable

Explicit Operator Splitting Methods

1. MBE

$$u_t = -\delta\Delta^2 u - \nabla\cdot[(1-|\nabla u|^2)\nabla u]$$

$$u_t = \nabla\cdot[|\nabla u|^2\nabla u]$$

$\mathcal{S}_{\mathcal{N}}$ nonlinear

Strang splitting

$$u_t = -\Delta u - \delta\Delta^2 u$$

$\mathcal{S}_{\mathcal{L}}$ linear

Explicit Operator Splitting Methods

1. MBE

$$u_t = -\delta\Delta^2 u - \nabla\cdot[(1-|\nabla u|^2)\nabla u]$$

$$u_t = \nabla\cdot[|\nabla u|^2\nabla u] \quad \mathcal{S}_{\mathcal{N}} \text{ nonlinear}$$

Strang splitting

$$u_t = -\Delta u - \delta\Delta^2 u \quad \mathcal{S}_{\mathcal{L}} \text{ linear}$$

2. CH

$$u_t = -\delta\Delta^2 u + \Delta(u^3 - u)$$

$$u_t = \Delta(u^3) \quad \mathcal{S}_{\mathcal{N}} \text{ nonlinear}$$

Strang splitting

$$u_t = -\Delta u - \delta\Delta^2 u \quad \mathcal{S}_{\mathcal{L}} \text{ linear}$$

Linear $\mathcal{S}_{\mathcal{L}}$ $\quad u_t = -\Delta u - \delta \Delta^2 u$

Pseudo-Spectral method with fast-fourier transform (FFT algorithm):

$$\boxed{\begin{aligned} & u_t = -\Delta u - \delta \Delta^2 u \\ & \Omega = [0, L_x] \times [0, L_y] \end{aligned}} \xrightarrow{\text{FFT}} \boxed{\frac{d}{dt}\widehat{u}_{m,\ell}(t) = (r - \delta r^2)\widehat{u}_{m,\ell}(t)}$$

$$\xrightarrow{\text{exact solution}}$$

$$\boxed{\widehat{u}_{m,\ell}(t+\Delta t) = e^{(r-\delta r^2)\Delta t}\widehat{u}_{m,\ell}(t)} \xrightarrow{\text{IFFT}} \boxed{\{u_{j,k}(t+\Delta t)\}}$$

$$r = \left(\frac{2\pi m}{L_x}\right)^2 + \left(\frac{2\pi \ell}{L_y}\right)^2$$

Nonlinear $\mathcal{S}_{\mathcal{N}}$ (MBE) $u_t = \nabla \cdot [|\nabla u|^2 \nabla u]$

1-D case

$$u_t = (u_x^3)_x$$

We consider a uniform grid and introduce the following finite difference approximation of the $\frac{\partial}{\partial x}$ operator

- fourth-order approximation

$$(\psi_x)(x_j) = \frac{\psi_{j-2} - 8\psi_{j-1} + 8\psi_{j+1} - \psi_{j+2}}{12\Delta x} + \mathcal{O}\left((\Delta x)^4\right)$$

- can be generalized to $2m^{th}$-order using central-difference

For 2-D case:

$$u_t = \nabla \cdot [|\nabla u|^2 \nabla u]$$

$$u_t = \left((u_x)^3 + (u_y)^2 u_x\right)_x + \left((u_x)^2 u_y + (u_y)^3\right)_y$$

We consider a uniform grid, and introduce the following $2m^{th}$-order finite difference approximation of the $\frac{\partial}{\partial x}$ and $\frac{\partial}{\partial y}$ operators

- fourth-order approximation

$$\psi_x(x_j, y_k) = \frac{\psi_{j-2,k} - 8\psi_{j-1,k} + 8\psi_{j+1,k} - \psi_{j+2,k}}{12\Delta x} + \mathcal{O}((\Delta x)^4)$$

$$\psi_y(x_j, y_k) = \frac{\psi_{j,k-2} - 8\psi_{j,k-1} + 8\psi_{j,k+1} - \psi_{j,k+2}}{12\Delta y} + \mathcal{O}((\Delta y)^4)$$

- can be generalized to $2m^{th}$-order using central-difference

Physical Property (MBE)?

- Mass Conservation: automatically satisfied by using the flux form
- Energy Decay:

$$E(u) = \int_\Omega \left[\frac{\delta}{2}|\Delta u|^2 + \frac{1}{4}(|\nabla u|^2 - 1)^2 \right] d\boldsymbol{x} = E_{\mathcal{N}}(u) + E_{\mathcal{L}}(u)$$

where

$$E_{\mathcal{L}}(u) = \int_\Omega \left(\frac{\delta}{2}|\Delta u|^2 - \frac{1}{2}|\nabla u|^2 + \frac{1}{4} \right) d\boldsymbol{x}$$

$$E_{\mathcal{N}}(u) = \frac{1}{4} \int_\Omega |\nabla u|^4 \, d\boldsymbol{x}$$

Physical Property (MBE)?

- Mass Conservation: automatically satisfied by using the flux form
- Energy Decay:

$$E(u) = \int_\Omega \left[\frac{\delta}{2}|\Delta u|^2 + \frac{1}{4}(|\nabla u|^2 - 1)^2 \right] d\boldsymbol{x} = E_{\mathcal{N}}(u) + E_{\mathcal{L}}(u)$$

where

$$E_{\mathcal{L}}(u) = \int_\Omega \left(\frac{\delta}{2}|\Delta u|^2 - \frac{1}{2}|\nabla u|^2 + \frac{1}{4} \right) d\boldsymbol{x}$$

$$E_{\mathcal{N}}(u) = \frac{1}{4}\int_\Omega |\nabla u|^4 \, d\boldsymbol{x}$$

Physical Property (MBE)?

- Mass Conservation: automatically satisfied by using the flux form
- Energy Decay:

$$E(u) = \int_\Omega \left[\frac{\delta}{2}|\Delta u|^2 + \frac{1}{4}(|\nabla u|^2 - 1)^2\right] d\boldsymbol{x} = E_{\mathcal{N}}(u) + E_{\mathcal{L}}(u)$$

where

$$E_{\mathcal{L}}(u) = \int_\Omega \left(\frac{\delta}{2}|\Delta u|^2 - \frac{1}{2}|\nabla u|^2 + \frac{1}{4}\right) d\boldsymbol{x}$$

$$E_{\mathcal{N}}(u) = \frac{1}{4}\int_\Omega |\nabla u|^4 \, d\boldsymbol{x}$$

Theorem (Energy Decay Property in 1-D) The semi-discrete schemes satisfy the following energy decay property $\frac{d}{dt}E_{\mathcal{N}}^{\Delta} \leq 0$, where $E_{\mathcal{N}}^{\Delta}$ is a 1-D discrete version of the energy functional

$$E_{\mathcal{N}}^{\Delta} := \frac{1}{4}\sum_{j}(u_x)_j^4 \Delta x.$$

Theorem (Energy Decay Property in 2-D) The semi-discrete schemes satisfy the following energy decay property $\frac{d}{dt}E_{\mathcal{N}}^{\Delta} \leq 0$, where $E_{\mathcal{N}}^{\Delta}$ is a 2-D discrete version of the energy functional:

$$E_{\mathcal{N}}^{\Delta} := \frac{1}{4}\sum_{j}|\nabla_h u_{j,k}|^4 \Delta x \Delta y$$

with $\nabla_h u_{j,k} := ((u_x)_{j,k}, (u_y)_{j,k})^T$.

Nonlinear $\mathcal{S}_{\mathcal{N}}$ (CH)

$$u_t = \Delta(u^3) = \left((u^3)_x\right)_x + \left((u^3)_y\right)_y$$

We use the same grids and the same $2m^{th}$-order discrete approximation of the $\frac{\partial}{\partial x}$ and $\frac{\partial}{\partial y}$ operators as the MBE cases.

Nonlinear $\mathcal{S}_{\mathcal{N}}$ (CH)

$$u_t = \Delta(u^3) = \left((u^3)_x\right)_x + \left((u^3)_y\right)_y$$

Energy decay property?

$$E(u) = \int_\Omega \left[\frac{\delta}{2}|\nabla u|^2 + \frac{1}{4}(u^2-1)^2\right] d\boldsymbol{x} = E_{\mathcal{L}}(u) + E_{\mathcal{N}}(u)$$

$$E_{\mathcal{L}}(u) = \int_\Omega \left(\frac{\delta}{2}|\nabla u|^2 - \frac{1}{2}u^2 + \frac{1}{4}\right) d\boldsymbol{x} \qquad E_{\mathcal{N}}(u) = \frac{1}{4}\int_\Omega u^4\, d\boldsymbol{x}$$

Theorem (Energy Decay Property) The semi-discrete schemes satisfy the following energy decay property: $\frac{d}{dt}E_{\mathcal{N}}^{\Delta} \le 0$ where $E_{\mathcal{N}}^{\Delta}$ is a 2-D discrete version of the energy functional:

$$E_{\mathcal{N}}^{\Delta} := \frac{1}{4}\sum_j u_{j,k}^4 \Delta x \Delta y$$

ODE Solver

All the obtain ODE systems have to be solved numerically.

- Explicit ODE solvers: $\Delta t_{\mathrm{ODE}} \sim (\Delta x)^2$
- Implicit ODE solvers: unconditionally stable, the accuracy requirements would limit timestep size; Moreover, a large nonlinear algebraic system of equations has to be solved at each timestep

Our approach:

- *DUMKA3* [Medovikov; 1998]
  - explicit third-order large stability domain Runge-Kutta method
  - embedded formulas permit an efficient step size control
  - efficiency can be further improved when the Δt_{FE} is provided

Adaptive Splitting Time Step Δt

Efficiency of splitting methods: its ability to use large timesteps

- small Δt: the solution changes quite rapidly
- large Δt: solution is close to its steady state

To measure the solution variation - *roughness*:

$$w(t) = \sqrt{\frac{1}{|\Omega|}\int_\Omega [u(\boldsymbol{x},t) - \bar{u}(t)]^2\, d\boldsymbol{x}} \qquad \bar{u}(t) = \frac{1}{|\Omega|}\int_\Omega u(\boldsymbol{x},t)\, d\boldsymbol{x}$$

roughness-dependent monitor function [Qiao, Zhang, Tang; 2011]

$$\Delta t = \max\left(\Delta t_{\min},\ \frac{\Delta t_{\max}}{\sqrt{1+\alpha|w'(t)|^2}}\right), \quad \alpha = \text{constant}$$

$\Rightarrow$ a significant reduction of CPU time ($3 \sim 6$ times more efficient)

Example 1 – 1-D Morphological Instability

We first consider the 1-D MBE equation with $\delta = 1$ subject to the initial condition

$$u(x,0) = 0.1\left(\sin\frac{\pi x}{2} + \sin\frac{2\pi x}{3} + \sin \pi x\right), \quad x \in [0,12].$$

This example was studied in [Li, Liu; 2003] to observe the morphological instability due to the nonlinear interaction.

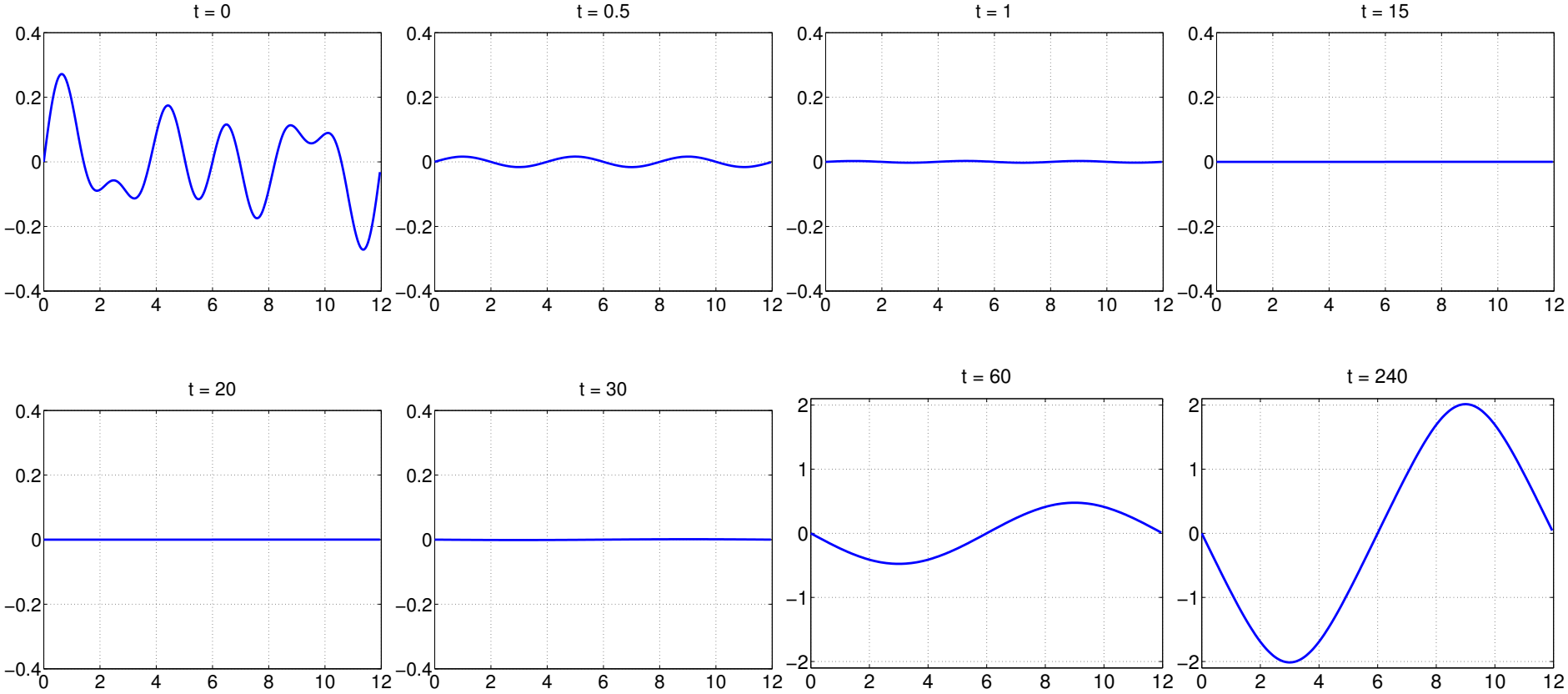

Example 1: u computed with constant splitting step $\Delta t = 10^{-1}$.

Compared to the results reported in [Li, Liu; 2003], our steady state is in a good agreement with the one obtained there, while the "buffering" time evolution is very different.

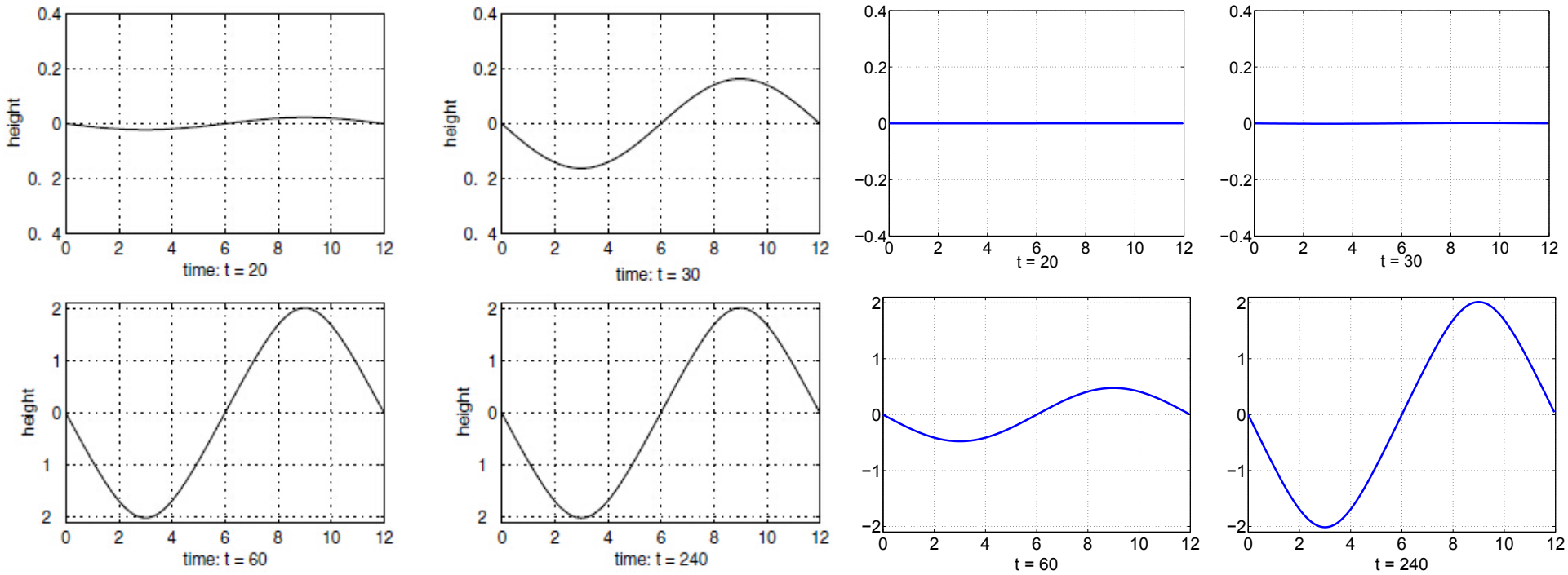

Left: [Li, Liu; 2003]; Right: our computation.

Difference in "buffering" time?

Compared to the results reported in [Li, Liu; 2003], our steady state is in a good agreement with the one obtained there, while the "buffering" time evolution is very different.

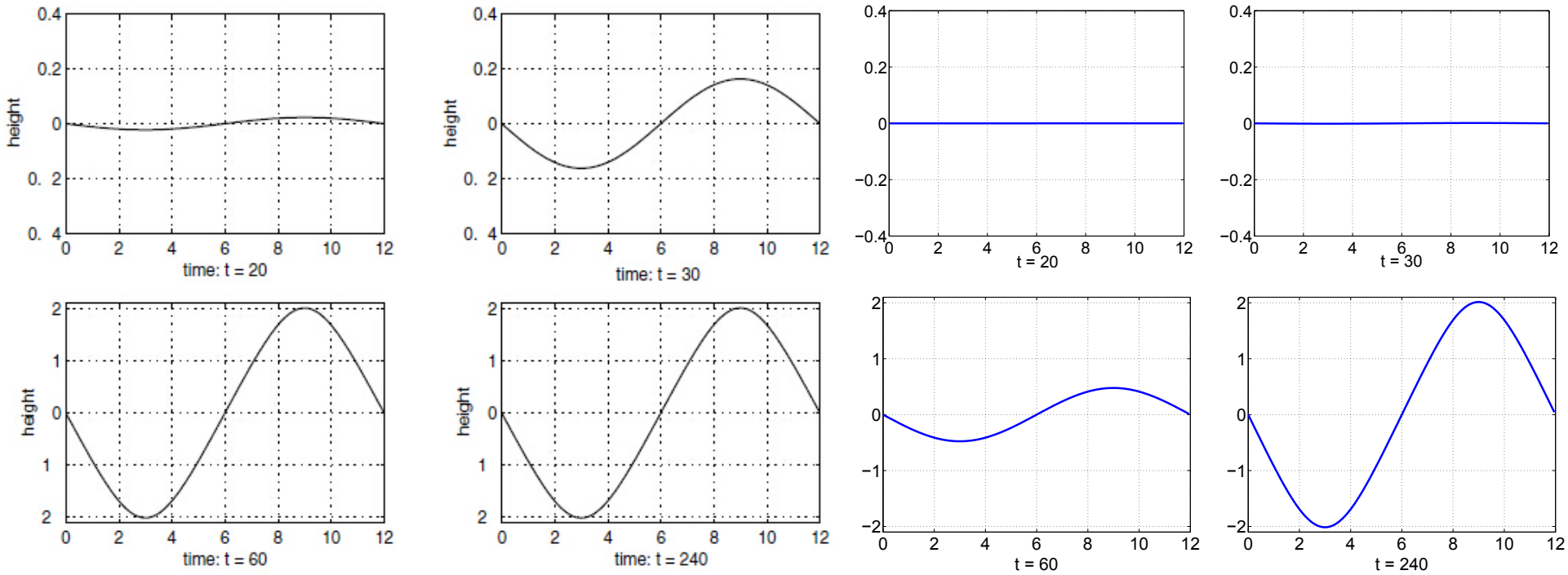

Left: [Li, Liu; 2003]; Right: our computation.

Difference in "buffering" time?

- reduce the splitting step: $\Delta t = 10^{-2}$
- adaptive strategy: $\Delta t_{\max} = 10^{-1}$ $\Delta t_{\min} = 10^{-2}$ $\alpha = 10^{3}$

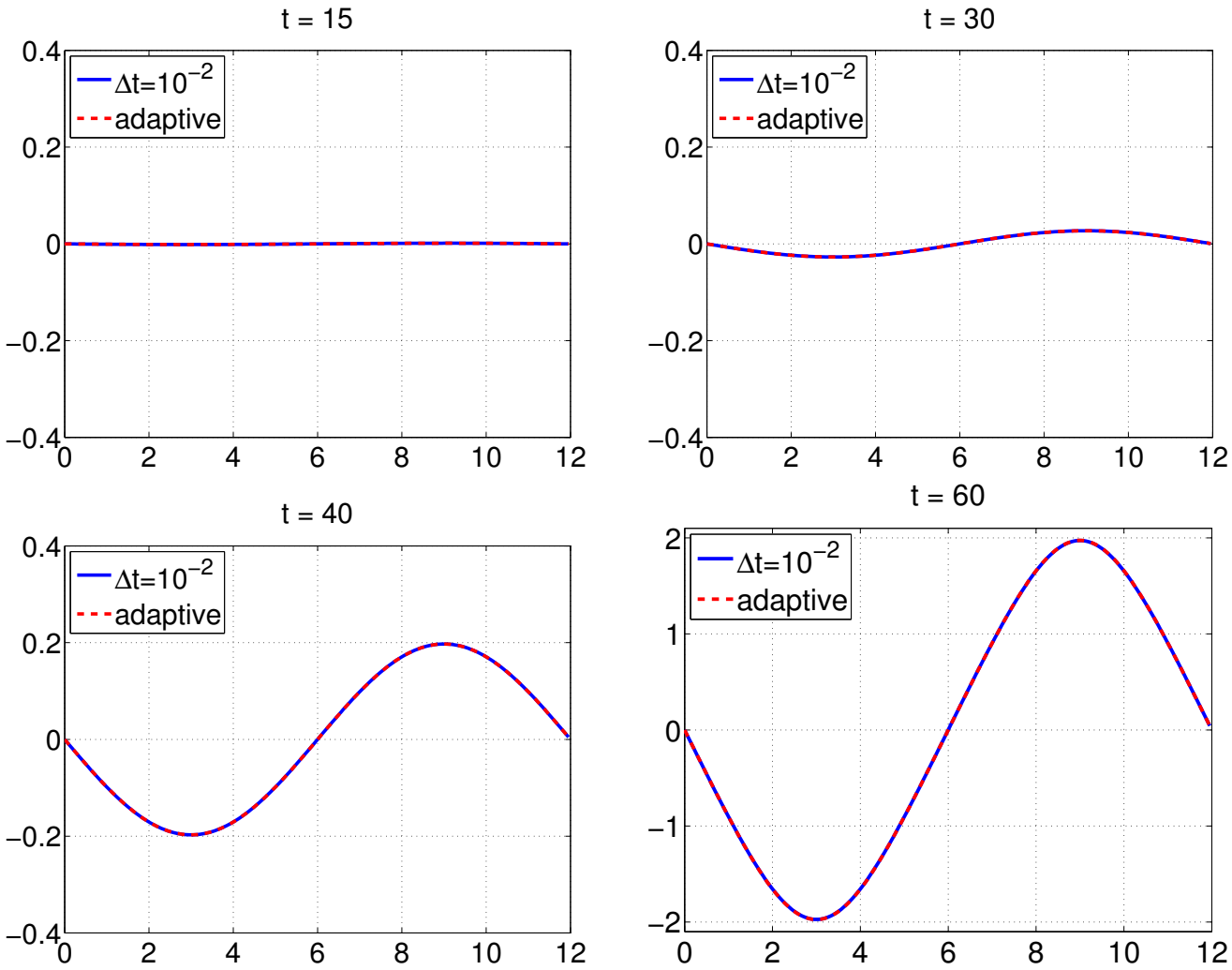

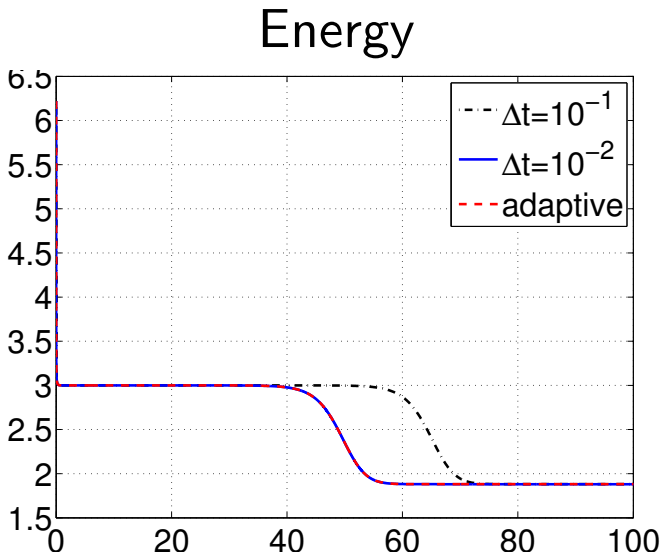

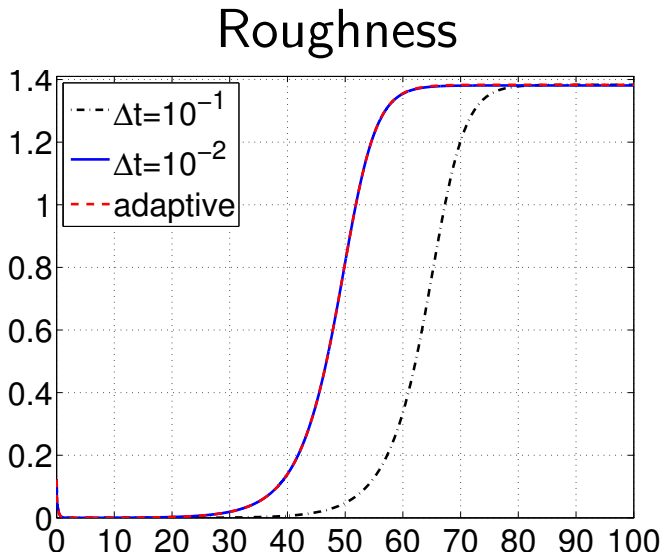

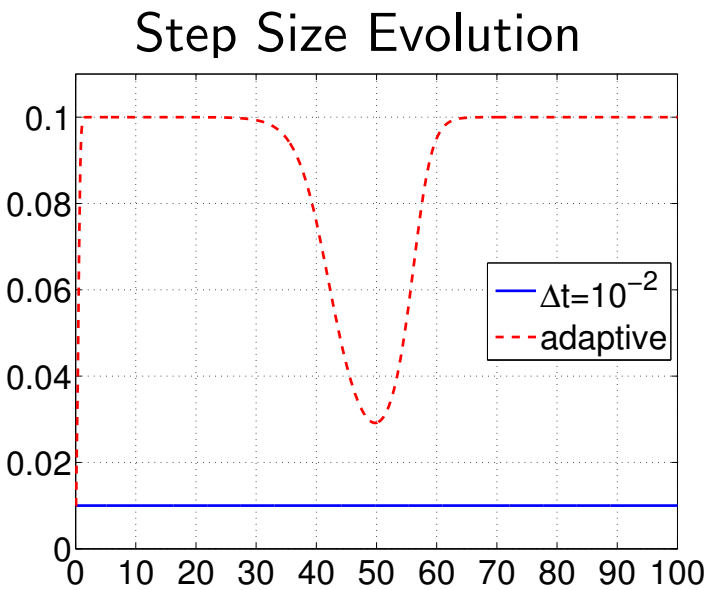

- Adaptive strategy:

$$\Delta t_{\min} = 10^{-2} \quad \Delta t_{\max} = 10^{-1}$$

$$\alpha = 10^3$$

N	T	Splitting step	CPU time
256	240	constant	3.2805
		adaptive	0.9659

Example 1 (conti.) – Accuracy Test

- Experimental convergence rate is close to the expected second-order

N	Δt	$\|\|u^{N,\Delta t} - u^{N/2,2\Delta t}\|\|_1$	Rate	$\|\|u^{N,\Delta t} - u^{N/2,2\Delta t}\|\|_\infty$	Rate
128	2e-2	3.95e-03	–	7.58e-04	–
256	1e-2	1.07e-03	1.89	2.45e-04	1.63
512	5e-3	2.73e-04	1.97	7.17e-05	1.78
1024	2.5e-3	6.84e-05	1.99	1.93e-05	1.89

- Fix $\Delta t = 10^{-3}$: the experimental convergence rate is fourth-order $\Rightarrow$ fourth-order finite-difference scheme. (small splitting error $\varepsilon^3(\Delta t^2)$)

N	Δt	$\|\|u^{N,\Delta t} - u^{N/2,\Delta t}\|\|_1$	Rate	$\|\|u^{N,\Delta t} - u^{N/2,\Delta t}\|\|_\infty$	Rate
128	1e-3	8.06e-05	–	2.25e-05	–
256	1e-3	5.18e-06	3.96	1.44e-06	3.96
512	1e-3	3.27e-07	3.99	9.10e-08	3.99
1024	1e-3	2.02e-08	4.02	5.62e-09	4.02

Example 1 (conti.) – Accuracy Test

- Experimental convergence rate is close to the expected second-order

N	Δt	$\|\|u^{N,\Delta t} - u^{N/2,2\Delta t}\|\|_1$	Rate	$\|\|u^{N,\Delta t} - u^{N/2,2\Delta t}\|\|_\infty$	Rate
128	2e-2	3.95e-03	–	7.58e-04	–
256	1e-2	1.07e-03	1.89	2.45e-04	1.63
512	5e-3	2.73e-04	1.97	7.17e-05	1.78
1024	2.5e-3	6.84e-05	1.99	1.93e-05	1.89

- Fix $\Delta t = 10^{-3}$: the experimental convergence rate is fourth-order $\Rightarrow$ fourth-order finite-difference scheme. (small splitting error $\varepsilon^3(\Delta t^2)$)

N	Δt	$\|\|u^{N,\Delta t} - u^{N/2,\Delta t}\|\|_1$	Rate	$\|\|u^{N,\Delta t} - u^{N/2,\Delta t}\|\|_\infty$	Rate
128	1e-3	8.06e-05	–	2.25e-05	–
256	1e-3	5.18e-06	3.96	1.44e-06	3.96
512	1e-3	3.27e-07	3.99	9.10e-08	3.99
1024	1e-3	2.02e-08	4.02	5.62e-09	4.02

Example 2 – 2-D Morphological Instability

We consider the 2-D MBE equation with $\delta = 0.1$ subject to the following initial condition:

$$u(\boldsymbol{x}, 0) = 0.1(\sin 3x \sin 2y + \sin 5x \sin 5y), \quad \boldsymbol{x} \in [0, 2\pi]^2$$

This example was studied in [Li, Liu; 2003] [Xu, Tang; 2006] to observe the morphological instability due to the nonlinear interaction.

We compute the solution on a 256×256 uniform grid with the constant splitting step $\Delta t = 10^{-3}$. Contour plots of the height profiles:

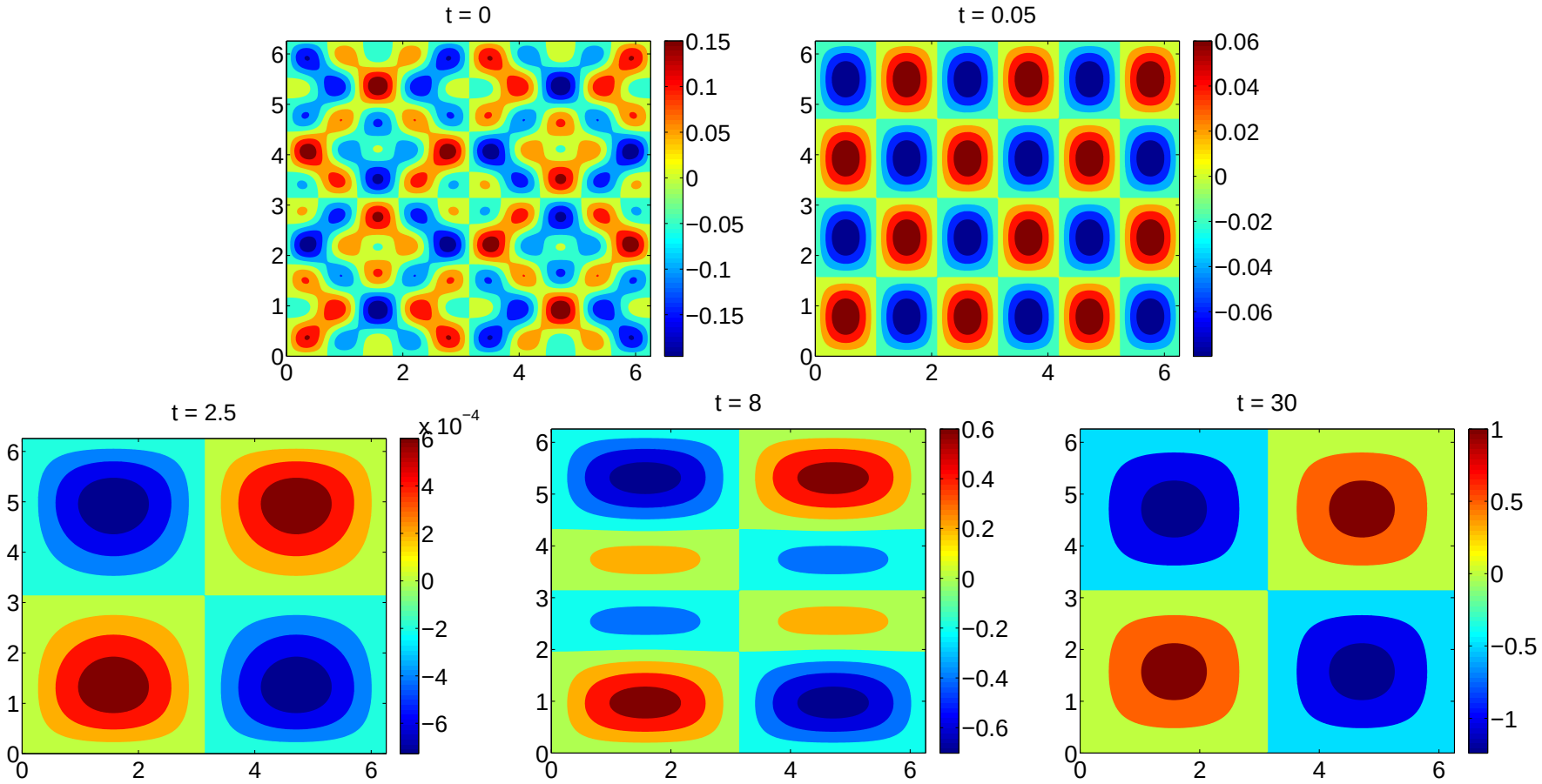

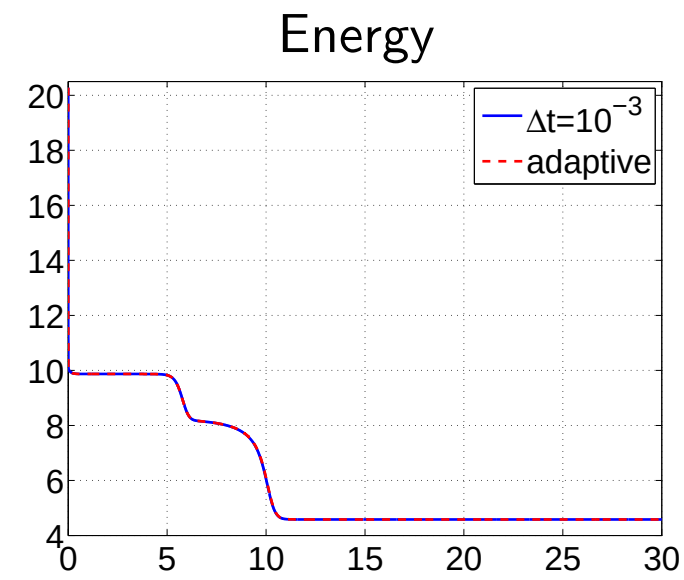

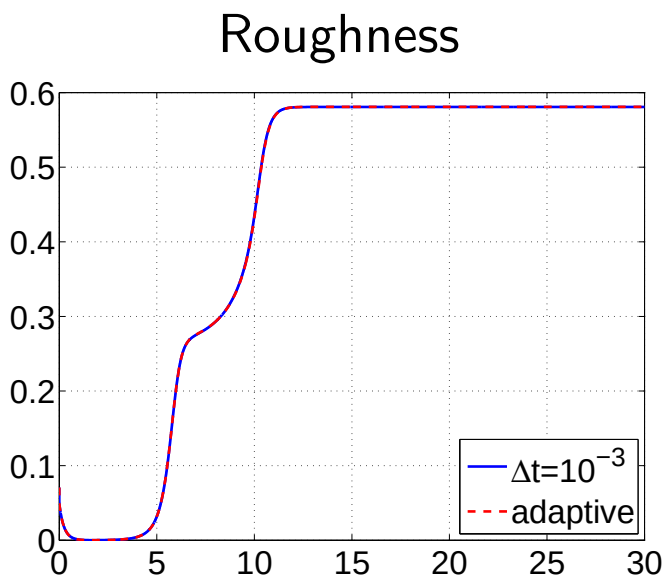

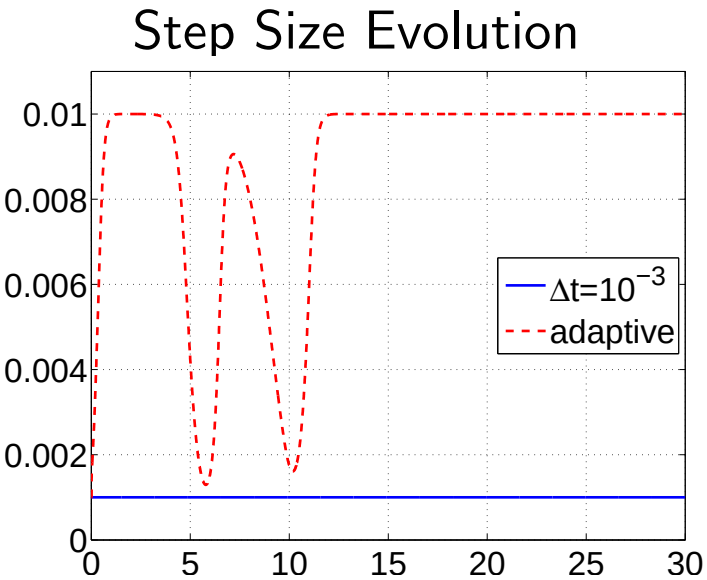

- Adaptive strategy:

$$\Delta t_{\min} = 10^{-3} \quad \Delta t_{\max} = 10^{-2}$$

$$\alpha = 10^3$$

N	T	Splitting step	CPU time
256	30	constant	4601.9
		adaptive	838.9

Example 2 (conti.) – Accuracy Test

Finally, we perform the mesh-refinement study and verify the experimental convergence rates are close to the expected second-order one.

N	Δt	$\|\|u^{N,\Delta t} - u^{N/2,2\Delta t}\|\|_1$	Rate	$\|\|u^{N,\Delta t} - u^{N/2,2\Delta t}\|\|_\infty$	Rate
64	4e-3	3.36e-03	–	6.01e-04	–
128	2e-3	9.09e-04	1.88	1.55e-04	1.96
256	1e-3	2.48e-04	1.87	4.96e-05	1.64
512	5e-4	6.52e-05	1.93	1.55e-05	1.68

Example 3 – Coarsening Dynamics

In this example, we study the 2-D MBE equation with $\delta = 1$ subject to random initial data:

- assign a uniformly distributed random number in the range $[-0.001, 0.001]$ to each grid point value of $u(\boldsymbol{x}, 0)$
- use a 512×512 uniform grid on the computational domain $\Omega = [0, 1000]^2$

Example 3 – Coarsening Dynamics

In this example, we study the 2-D MBE equation with $\delta = 1$ subject to random initial data:

- assign a uniformly distributed random number in the range $[-0.001, 0.001]$ to each grid point value of $u(\boldsymbol{x}, 0)$
- use a 512×512 uniform grid on the computational domain $\Omega = [0, 1000]^2$

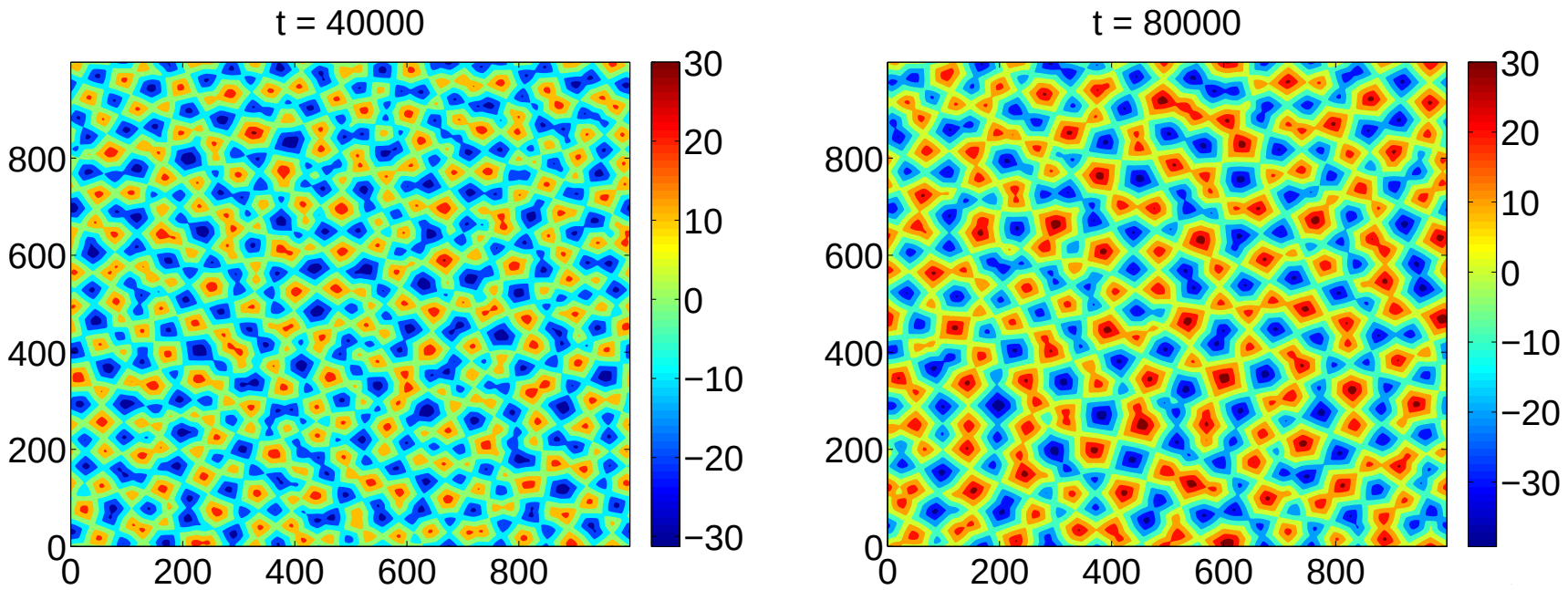

Free energy function

$$F_{free} := \frac{1}{4}(|\nabla u| - 1)^2 + \frac{\delta}{2}|\Delta u|^2$$

- free energy is concentrated on edge
- could be used to identify the edges of the pyramidal structures

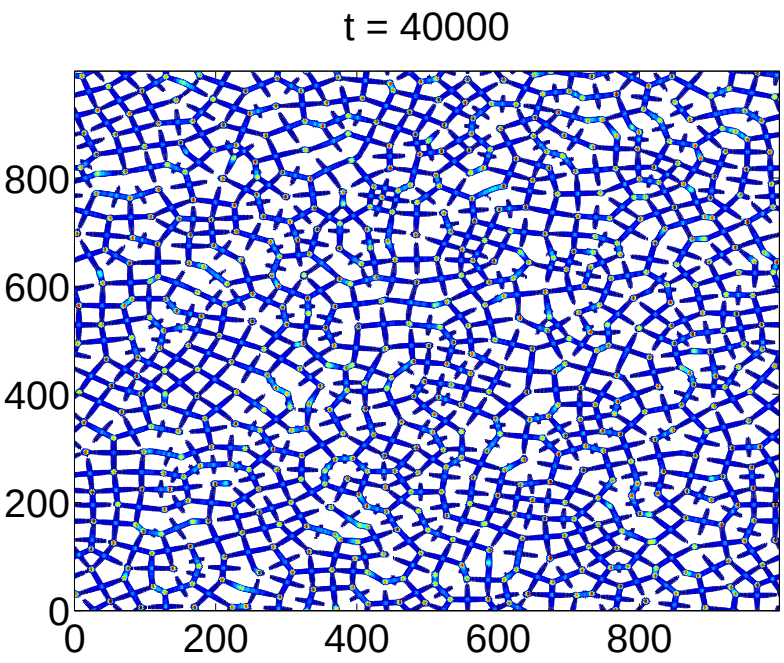

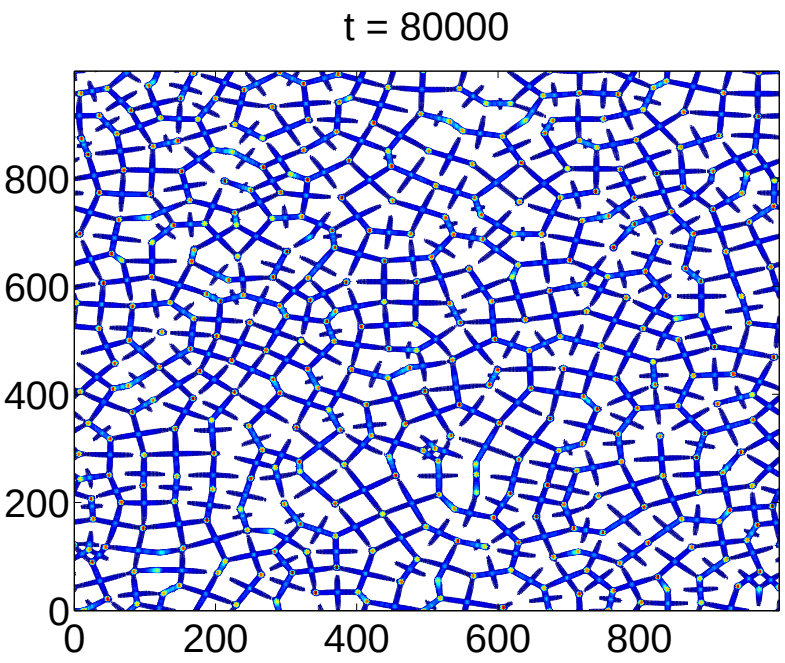

We present the log-log scale plot of the interface height $\tilde{u}(t) = \sqrt{\frac{1}{|\Omega|}\int_\Omega u^2(\boldsymbol{x},t)\,d\boldsymbol{x}}$ and the evolution of the mean height $\bar{u}(t)$:

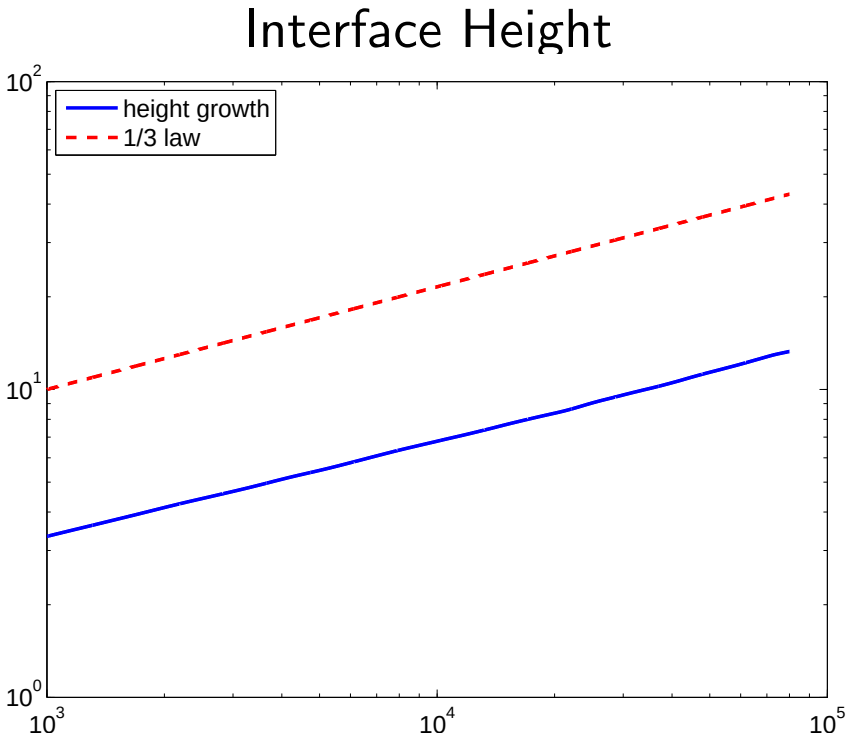

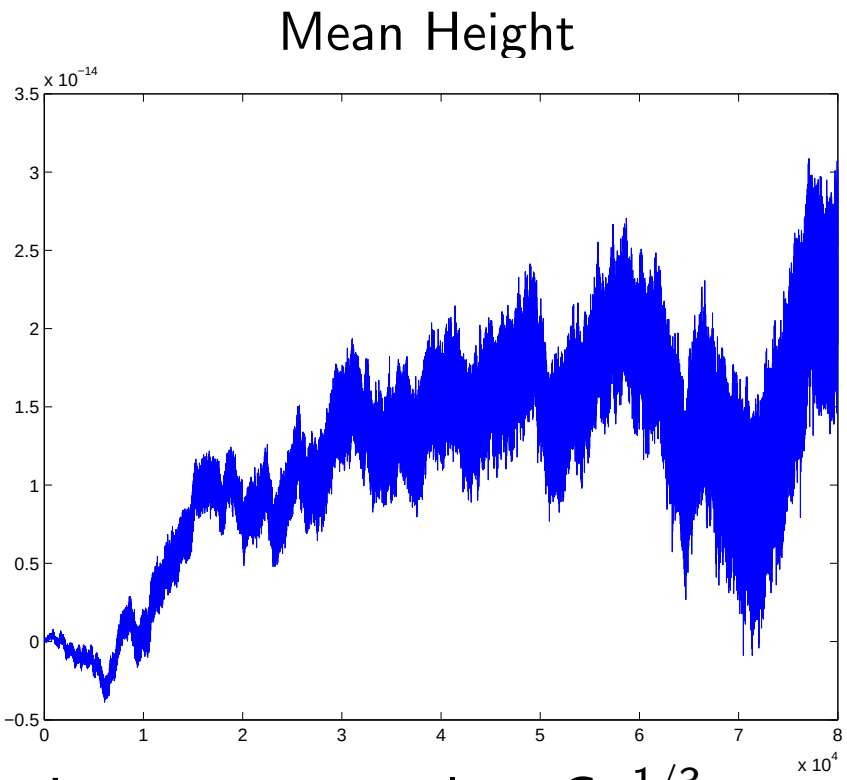

- The height of the pyramids grow in time as a power law $C\,t^{1/3}$.
- The difference $\bar{u}(t) - \bar{u}(0)$ remains practically zero at all times $\Rightarrow$ mass conservation.

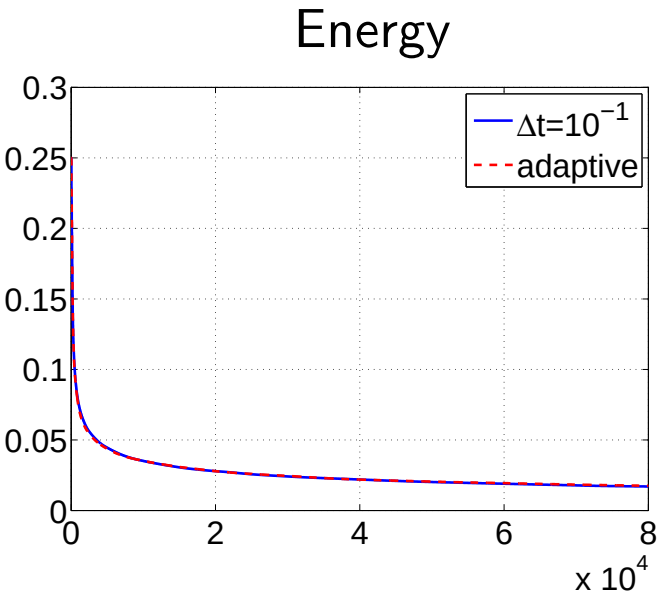

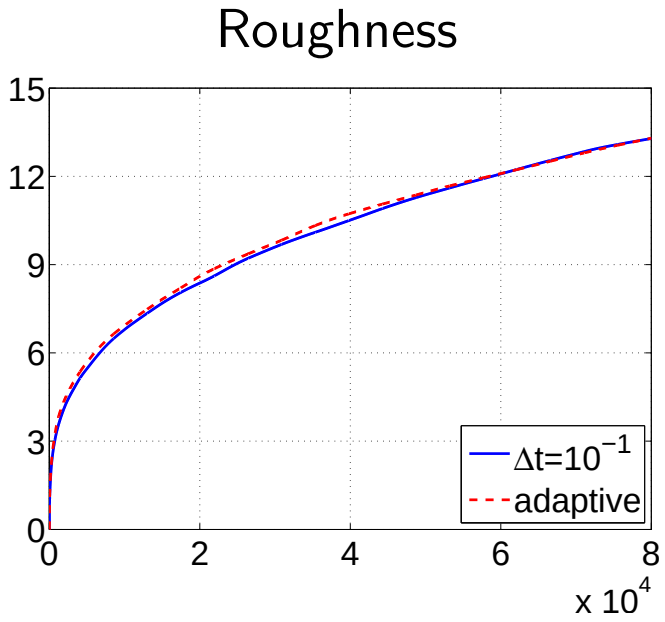

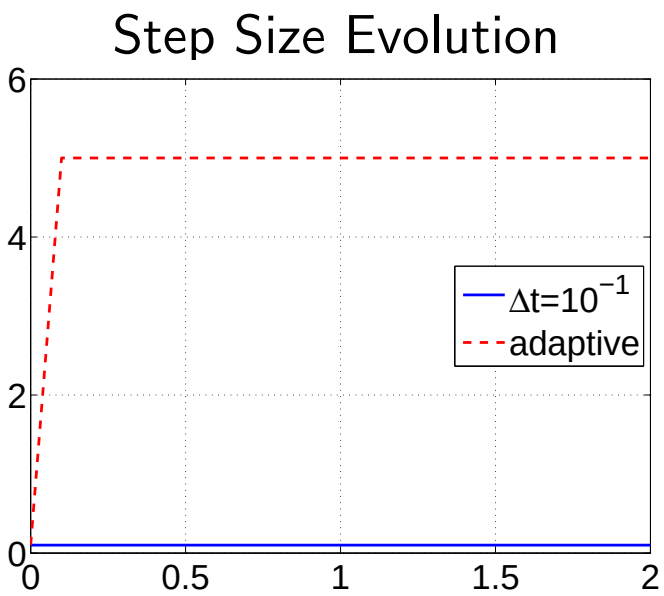

- Adaptive strategy:

$$\Delta t_{\min} = 10^{-1} \quad \Delta t_{\max} = 5$$

$$\alpha = 1$$

N	T	Splitting step	CPU time
512	80000	constant	223370
		adaptive	38775

Example 4 – Phase Separation

In this example, taken from [Feng, Tang, Yang; 2015], we consider the 2-D CH equation with $\delta = 0.01$ subject to the following non-mean-zero initial condition:

$$u(\boldsymbol{x}, 0) = 0.05 \sin x \sin y + 0.001, \quad \boldsymbol{x} \in [0, 2\pi]^2$$

- 128×128 uniform grid
- constant splitting step $\Delta t = 10^{-3}$

- constant step $\Delta t = 10^{-3}$ (upper)
- Adaptive strategy: $\Delta t_{\min} = 10^{-3},\ \Delta t_{\max} = 10^{-2},\ \alpha = 10^{2}$ (lower)

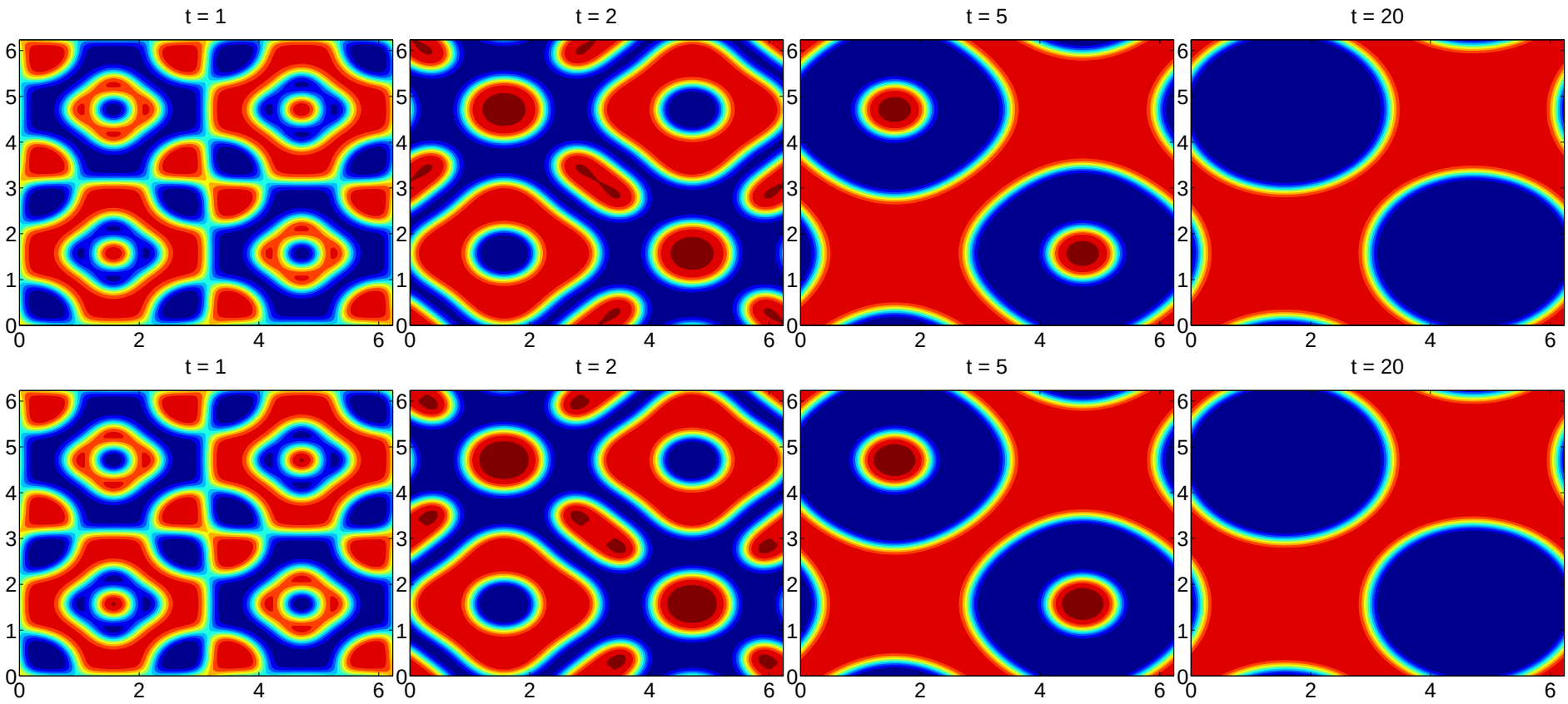

The solution dynamics can be captured correctly when the adaptive strategy is employed.

Energy

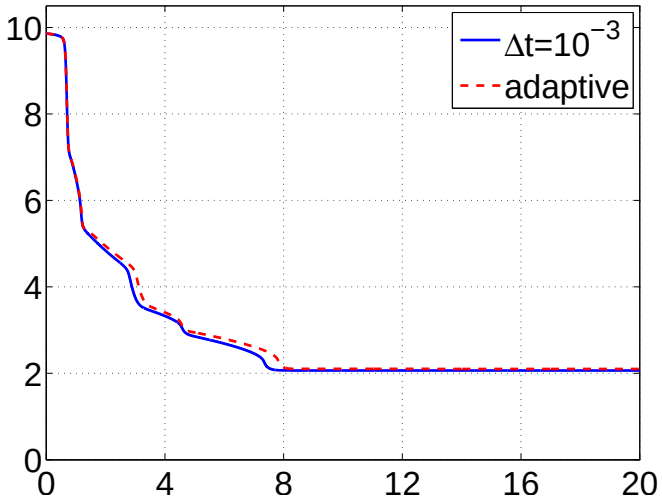

Roughness

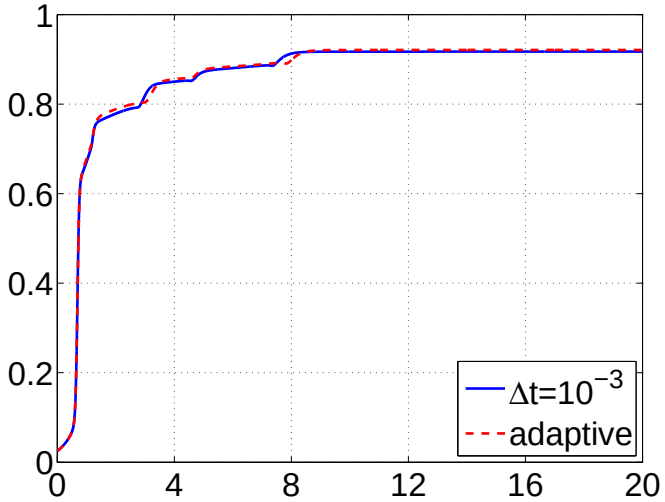

Step Size Evolution

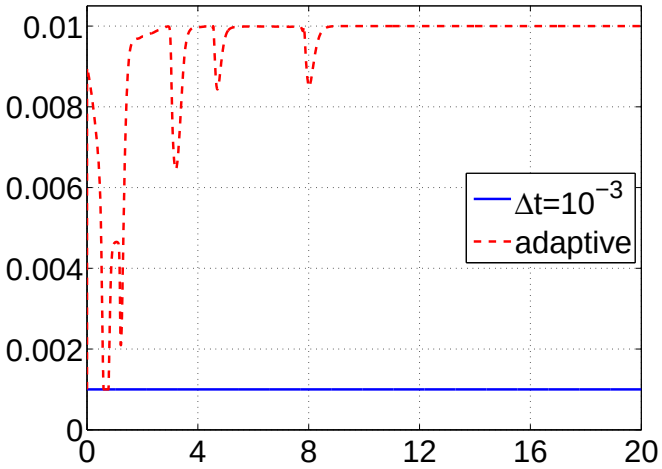

- Adaptive strategy:

$$\Delta t_{\min} = 10^{-3} \quad \Delta t_{\max} = 10^{-2}$$

$$\alpha = 10^2$$

N	T	Splitting step	CPU time
128	20	constant	504.09
		adaptive	125.86

Thanks for your attention.

Hyperbolic System of Conservation Law

$$u_t + f(u)_x = 0$$

- with the nonlinear flux function $f(u)$
- it admits non-smooth solutions (shocks and rarefaction waves)
- even when a smooth initial condition is prescribed
- shock capturing methods

Godunov-Type Central-Upwind Schemes

The second-order Godunov-type central-upwind schemes

- a finite-volume based hyperbolic solver
- simple, robust, Riemann-problem-solver-free, yet high-resolution methods
- can be used as as "black-box" solvers for general (multidimensional) hyperbolic systems of conservation laws

Reference

- Kurganov, Lin. On the reduction of numerical dissipation in central-upwind schemes, *Commun. Comput. Phys.* 2007
- Kurganov, Noelle, Petrova. Semidiscrete central-upwind schemes for hyperbolic conservation laws and Hamilton-Jacobi equations, *SIAM J. Sci. Comput.* 2001
- Kurganov, Tadmor. New high resolution central schemes for nonlinear conservation laws and convection-diffusion equations, *J. Comput. Phys.* 2000

Third-Order Strong-Stability Preserving Runge-Kutta (SSP-RK) ODE solver

Features

- maintain the strong stability property (TVD)
- achieve higher order accuracy in time
- the four-stage, fourth-order SSP RungeCKutta scheme with a nonzero CFL coefficient must have at least one negative coefficient

Reference

- Gottlieb, Ketcheson, Shu. *Strong stability preserving Runge-Kutta and multistep time discretizations.* 2011
- Gottlieb, Shu, Tadmor. Strong Stability-Preserving High-Order Time Discretization Methods. *SIAM Rev.* 2001

DUMKA3 ODE Solver

Features

- It is based on a family of explicit Runge-Kutta-Chebyshev formulas of order three
- It uses optimal third order accuracy stability polynomials with the largest stability region along the negative real axis
- The embedded formulas permit an efficient stepsize control

Reference

- Medovikov. High order explicit methods for parabolic equations. *BIT*, 1998.
- Abdulle and Medovikov. Second order chebyshev methods based on orthogonal polynomials. *Numerische Mathematik* 2001
- http://dumkaland.org/

Phase Separation

- Energy

$$E(u) = \int_\Omega \left[\frac{\delta}{2}|\nabla u|^2 + \frac{1}{4}(u^2-1)^2\right] d\boldsymbol{x}$$

  decays to zero.
- Example: Phase Separation in Gasolines containing Ethanol (when water comes in): the Ethanol will pick-up and absorb some or all of water. When it reaches a saturation point the Ethanol and water will Phase Separate, actually coming out of solution and forming two or three distinct layers in the tank.
- Thermodynamic equilibrium: the entropy is maximized, free energy is minimized